Exploring Geochemical Methods to Measure Arsenic-Dissolved Organic Matter Complexes and Coal Combustion Residuals in Surface Water

by

Caitlyn Herron

A thesis submitted to the Graduate Faculty of
Auburn University
in partial fulfillment of the Requirements
for the Degree of Geology, Master of Science

Auburn, Alabama
December 10, 2022

Keywords: arsenic, dissolved organic matter, complexation, coal combustion residuals

Copyright 2022 by Caitlyn Herron

Approved by

Dr. Ann Sullivan Ojeda, Assistant Professor, Geoscience
Dr. Ming-Kuo Lee, Chair, Geoscience
Dr. Yaniv Olshansky, Assistant Professor, Geoscience

Abstract

Chapter 1, investigates the geochemical controls governing arsenic (As) mobility, precisely the formation of As-DOM complexes. Dissolved organic matter (DOM) reduces As mobility through equilibrium binding of As to the outer and/or inner sphere of DOM, creating an As-DOM complex (Buschmann et al., 2006; Ren et al., 2017; Tipping, 2002). Conversely, DOM increases As mobility if(1) As binding in the As-DOM complex is reversible, (2) the DOM structure is degraded, (3) there is competitive sorption where DOM will preferentially bind to a mineral surface, inhibiting As binding, and (4) the complex remains soluble in solution (Dowling et al., 2002; Liu and Cai, 2010; Miller et al., 2010; Redman, 2002). To determine As-DOM complex formation, two separate methods were utilized (1) high performance liquid chromatography (HPLC), size exclusion column separation (SEC), inductively coupled mass plasma spectroscopy (ICP-MS), ultra-violet visible spectroscopy (UV-VIS), and fluorescence detection (FLD) and (2) equilibrium dialysis experiments. Additional methods, including spectroscopic methods and functional group quantification, were employed to investigate trends between DOM characteristics and As complexation capacity. Lignite derived DOM was utilized to compare metal binding capacity between the lignite derived DOM and a known DOM standard, Suwannee River Natural Organic Matter (SRNOM).

In HPLC-SEC-ICP-MS analysis, a complexed As peak was observed at 17 across all DOM types; a free As peak was observed at 28 minutes across all DOM types and ultra-pure water. Three independent lines of evidence was produced to confirm the detection of free and complexed As: (1) free As elutes later than complexed As which is consistent with SEC theory and (2) HPLC-SEC-FLD analysis and (3) HPLC-SEC-UV analysis produced peaks at a similar retention time, 28 minutes. In both HPLC-SEC-ICP-MS and equilibrium dialysis results, log K_D results decreased with increased addition of As which is likely caused by the saturation of As and loss of DOM complexation sites. A larger As-DOM complex, at minute 13, was also identified with lignite derived DOM samples. This study confirmed the use of HPLC-SEC-ICP-MS as a precise tool for determining As-DOM complexes; HPLC-SEC-ICP-MS results were comparable to previous literature and those calculated through equilibrium dialysis. We recommend that future studies focus on the use of HPLC-SEC-ICP-MS to gather more detailed information regarding the molecular characteristics of DOM fraction responsible for complexation. HPLC-SEC-ICP-MS analysis suggests that lignite derived DOM has a larger complexation capacity compared to the DOM standard, SRNOM, implying that complexation may be underestimated in groundwater systems in previous literature.

The second study, Chapter 2, investigated coal combustion residual (CCR) contamination at two samples sites, Gadsden, and Gaston impoundments, along the Coosa River in Alabama. CCR is created as a byproduct of coal combustion at electrical powerplants and stored in CCR impoundments across the United States (Wang et al., 2020). CCR contamination produces an enrichment in heavy metals in sediments and surface water after decades of potential contamination in shallow aquifers and flood events (Aguirre, 2019; Harkness et al., 2016; Vengosh et al., 2019; Wang et al., 2019). The research objective of this study was to evaluate the impact of CCR impoundments on the nearby sediment and water quality. Seven samples were collected in proximity to Gadsden impoundment and seven samples collected near the Gaston impoundment. Heavy metal enrichment of surface water and sediment samples were utilized as a diagnostic tool for CCR contamination. The linear relationship between molybdenum (Mo) and antimony (Sb) was also employed as additional evidence. Sediment and surface water produced a similar

enrichment pattern as one produced in previous literature, however most elements studied had an enrichment value below 10. A strong linear relationship between Mo and Sb was found in both sediment (R^2=0.8758) and surface water samples (R^2=0.8215). The evidence is inconclusive to suggest that CCR contamination is contributing to reduced water quality in the Coosa River.

Acknowledgments

I need to initially thank my advisor, Dr. Ann Ojeda, for all her support and mentorship throughout my time at Auburn. In research endeavors and life, unexpected challenges test the limits of the human spirit. I was lucky to have had the unwavering support of Dr. Ojeda as I overcame both.

I would like to thank my other committee members, Dr. Lee and Dr. Olshanksy, for their input and guidance support throughout the project. I am grateful for the support of Dr. Lee's lab especially the assistance of Dr. Zeki Billor with ICP-MS and HPLC-SEC-ICP-MS analysis. This project could not have been completed without the financial support for this project through the 2021 Water Resource Competitive Grants Program from the Alabama Water Resource Research Institute.

I am grateful for the collaboration and support of the Ojeda Contaminant lab. Your input and camaraderie have been invaluable. This thesis could not have been completed without the assistance of Dr. Natalia Malina. Dr. Malina has not only been a source of guidance and collaboration but a friend. Thank you for going above and beyond. I will never forget our late nights in CASIC together.

A special thanks to my friends and family for your unwavering support and love throughout the years. Thank you, Ella and Mallory, for all the advice, support, laughs, and edits.

This work is dedicated to my husband, John.

Table of Contents

List of Figures

List of Tables

List of Abbreviations

DOM	Dissolved Organic Matter
As	Arsenic
HPLC	High Performance Liquid Chromatography
ICP-MS	Inductively Coupled Plasma Mass Spectroscopy
SEC	Size Exclusion Chromatography
UVVIS/UV	Ultraviolet-visible spectroscopy
SRNOM	Suwannee River Natural Organic Matter
DH	Coal Extract Sample from Dolet Hills, Louisiana
HS	Coal Extract Sample from Hot Springs County, Arkansas
Fe	Iron
CCR	Coal Combustion Residuals
Mo	Molybdenum
Sb	Antimony
Se	Selenium
BDL	Below Detection Limit

Preface

Water quality is a pressing issue for many communities around the world as reduced water quality threatens the health and welfare of communities that are dependent on those water resources. This work encloses two chapters investigating two independent water quality issues, As mobility and CCR contamination. Chapter 1, Arsenic-Dissolved Organic Matter Complexation: A Comparison of Equilibrium Dialysis and HPLC-SEC-ICP-MS Analysis, explores the geochemical reactions constraining As mobility. We use a range of analytical techniques precisely detect As-DOM complexes and the trends related to their formation. Chapter 2, Investigation of Coal Combustion Residuals Contamination in Alabama: A Coosa River Example, examines the Coosa River for potential CCR contamination. Environmental samples were collected in the Coosa and inspected for diagnostic signatures of CCR contamination.

Chapter 1: Arsenic-Dissolved Organic Matter Complexation: A Comparison of Equilibrium Dialysis and HPLC-SEC-ICP-MS Analysis

1.1 Introduction

Arsenic (As) contamination is a worldwide risk to groundwater resources. As can originate from both geogenic sources like aquifer materials and soils as well as anthropogenic sources like arsenical herbicides (Nordstrom, 2002). In Bangladesh, an estimated 39 million people are exposed to As concentrations above the World Health Organization guideline of 10 µg/L in drinking water (Progotir Pothey, 2015). Termed the "world's greatest mass poisoning", the situation in West Bengal is only one of many regions that experience geogenic As contamination. Globally, As in groundwater is documented in Argentina, Austria, Brazil, Canada, China, Ghana, Greece, Hungary, Iceland, India, Japan, Korea, Malaysia, Mexico, Mongolia, Nepal, Romania, Taiwan, Vietnam, Zimbabwe, and the United States (Selinus, 2013). In the United States, approximately 2 million people depend on private wells and 11% of public water supplies are expected to have As concentrations above the US Environmental Protection agency limit of 10 µg/L (Ayotte et al., 2017; Focazio et al., 2000). Chronic exposure to As in drinking water is linked to cancer of the lung, bladder, and skin (National Research Council (US) Committee on Medical and Biological Effects of Environmental Pollutants, 1977). Therefore, understanding geochemical controls on arsenic mobility in groundwater is critical to protect human health and wellbeing.

In the environment, As mobility is controlled through multiple geochemical processes. Geochemical controls generally include (1) reductive dissolution and desorption, (2) pH-driven desorption, (3) ion concentration in low recharge areas, and (4) ion competition (Smedley and Kinniburgh, 2002). Recently, As mobility has been tied to the concentration and chemical characteristics of dissolved organic matter (DOM). DOM can reduce As mobility through

equilibrium binding of As to the outer sphere and/or inner sphere of DOM, creating As-DOM complexes (Buschmann et al., 2006; Ren et al., 2017; Tipping, 2002). Conversely, DOM increases As mobility if (1) As binding in the As-DOM complex is reversible, (2) the DOM structure is degraded, (3) competitive sorption so that DOM preferentially binds to the mineral surface, inhibiting As binding, and (4) the complex remains soluble (Dowling et al., 2002; Liu and Cai, 2010; Miller et al., 2010; Redman, 2002). The formation of As-DOM complexes has been documented by multiple studies (Bauer and Blodau, 2009; Buschmann et al., 2006; Liu et al., 2011; Liu and Cai, 2014, 2010; Ritter et al., 2006; Warwick et al., 2005).

The diversity in sources and molecular structure of DOM make DOM and As-DOM complexes difficult to characterize. A single water sample can contain thousands of different DOM molecules and identifying precise molecular structures is exceedingly difficult (Kalbitz et al. 2003, Ide et al. 2017, Kim et al. 2003, Wozniak et al. 2008). An alternative approach has been to characterize chemical functional groups and bulk spectroscopic properties that relate to DOM reactivity in the environment. For example, DOM is often characterized by the extent of aromatization and quantifying phenolic and carboxylic functional groups, which are directly involved in metal-DOM complexation. Bulk spectral properties are typically determined through specific ultraviolet absorbance ($SUVA_{254}$) and potentiometric acid-base titrations (Stevenson, 1994; Tipping, 2002; Weishaar et al., 2003). Changes in optical properties, either by quenching or enhancing optical signals, can serve as proxies for metal DOM-complexation (Gao et al., 2015; Tipping, 2002).

In groundwater systems, DOM structures are largely preserved as many of the degradation and alteration pathways are limited due to subsurface conditions (e.g. low light and redox potential) and lack of molecular oxygen (McDonough et al., 2022). Consequently, groundwater DOM is typically older with low oxygen/carbon (O/C) and high hydrogen/carbon (H/C) ratios

(McDonough et al., 2022). Differences in molecular structures of groundwater and surface water DOM present an issue for stakeholders utilizing DOM literature. The DOM reference standard, Suwannee River Natural Organic Matter (SRNOM), is surface water natural organic matter obtained from Suwannee River, Florida and isolated through reverse osmosis and groundwater DOM is rarely used in DOM modeling research. The scant understanding of groundwater DOM in literature raises questions on whether past research is representative of groundwater DOM cycling and metal-DOM complex formation in the subsurface.

Past studies have relied heavily on indirect measurements of As-DOM complexation based on spectroscopic methods or sequential filtration. Increases of DOC normalized differential spectrum with As addition can identify As-active chromophores as shown in Zhang et al., 2021. Differential spectra, the difference between an original spectra and an altered spectra, has been utilized to investigate DOM towered As binding (Li and Hur, 2017). Alternatively, As-DOM complexes quantified via filtration that rely on quantification of "free" As after a series of filtration steps and assume either the difference between "total" and "free" As must be the As-DOM complex. For example, As-DOM complexation has been inferred through nylon membrane filtrations with stages of molecular weight cut-offs (Warwick et al., 2005 and Bauer and Blodau, 2009) and through equilibrium dialysis experiments (Buschmann et al., 2006 and Ritter et al., 2006). Generally, these studies also assume a complete mass balance, which is sometimes, but not always, reported.

Direct evidence of As-DOM was observed in Liu et al., (2011), Liu and Cai, (2014), (2010) through an analytical technique that combined high performance liquid chromatography (HPLC), size exclusion column separation (SEC), inductively coupled mass plasma spectroscopy (ICP-MS), and UV-VIS detection. This technique employed SEC to separate "free" As and As-DOM

complexes by size while simultaneously detecting DOM and As with UV-VIS detector and ICP-MS, respectively. The set conditions for instrumentation of the HPLC-SEC-ICP-MS system are obstacles for investigating different environmental conditions that affect As-DOM complexation. The mobile phase required by the HPLC necessitates many experimental variables like salinity, dissolved oxygen, and redox conditions. However, direct measurements of As-DOM complexes provide multiple advantages: (1) no longer relying on inferring As-DOM complexation in the experiments (2) the size exclusion column provides information regarding the molecular weight of the colloid(s) responsible for complexation (3) the opportunity for measuring As-DOM complexes in environmental samples which is unattainable for past analytical methodology.

Although both HPLC-SEC-ICP-MS analysis and inferential techniques (e.g. dialysis experiments) have been used to quantify As-DOM complexation in past literature, a quantitative comparison of these methods is lacking. Therefore, the objective of this study was to quantify complexation of As with DOM through traditional dialysis experiments and HPLC-SEC-ICP-MS analysis. Furthermore, this study compared As-DOM complexation from surface water-derived DOM to that of groundwater-DOM to better understand the extent of As-DOM formation in groundwater systems.

1.2 Materials and Methods

1.2.1 Materials

All chemicals used in this study were of analytical grade. The chemicals used in this study included 3 M nitric acid (Ward's Science, USA), 1 M nitric Acid (Ward's Science, USA), sodium nitrate (VWR, USA), 0.1 M sodium metarsenite (Ricca Chemical, USA), potassium hydroxide (VWR, USA), and ammonium nitrate (Fischer, USA). As standards were prepared by diluting 0.1 M sodium metaarsenite to concentrations of 0.01, 0.001, and 0.00001 M sodium arsenite. All As standards were stored in high-density polyethylene bottles at 6 ºC until use.

The DOM sources included two lignite-derived DOM, described in more detail in 1.2.2, and Suwannee River Natural Organic Matter DOM (SRNOM) (2R101N, International Humic Substance Society, USA). All DOM solutions were diluted with ultrapure water to 25 mg/L TOC. Total organic carbon content was determined with a Shimadzu TOC-V combustion analyzer.

Dialysis tubes were purchased through VWR (Spectra/Pro Biotech Cellulose Ester membrane, 200 Da). Ultrapure water was used in all experiments (18Ω; Micropore System Thermo Scientific, USA).

1.2.2 Preparation of lignite-derived DOM

Two lignite samples originated from Dolet Hills, Louisiana (DH) and Hot Springs County, Arkansas (HS) were used in this study to simulate groundwater DOM. DOM stock solutions were prepared through a water-soluble extraction process described in Ojeda et al., (2019). Briefly, 8 grams of coal and 350 mL of ultrapure water were added to a 500 mL round-bottom flask attached to a water-jacket condenser. A stir bar was added, and the solution was heated to 80ºC for 72 hours. The solution was filtered with a Qualitative 410 Whatman filter paper and 0.45 µm cellulose

acetate filter. DOM stock solutions were acidified to a pH of 2 with 1 M nitric acid and kept at 6 ºC prior to complexation with As. Lignite is a geogenic material and contains low concentrations of arsenic. Background arsenic concentrations in the extracts were 3.03 µg/L for DH, 2.86 µg/L for HS, and 0.31 µg/L for SRNOM.

1.2.3 Absorbance Measurements

Two stock arsenite solutions of sodium arsenite (0.001M and 0.0001 M) were used with DOM solutions (25mg/L C) to create As-DOM solutions containing 0, 5, 10, 50, 100, 250, and 500 ppb As. Solutions were stored at 6 ºC for 24 hours to allow for complexation. After 24 hours, samples were analyzed using an Agilent Cary 2500 UV-Vis with a cell length of 1 cm scanning from 200 to 800 nm at 1 nm increments. $SUVA_{254}$ was calculated through the equation (EQ. 1) from Weishaar et al., 2003; the results are included in Figure 17 in the Appendix. Molar absorptivity coefficients were calculated using the Beer-Lambert law (EQ. 2).

$$SUVA_{254} = \frac{Absorbance\ _{254}(nm)}{DOC\ (mg)}\ x\ 100 \qquad \text{(EQ 1)}$$

$$Molar\ Absorptivity\ Coefficent = \frac{Absorbance}{path\ length\ (cm)\ Concentration\ (mg)} \qquad \text{(EQ 2)}$$

1.2.4 Functional Group Content

The functional group content, phenolic and carboxylic function groups, of each DOM type was quantified through potentiometric acid-base titrations described in Al-Reasi et al., (2013). Functional group content and titration curves of each DOM type is shown in Table 3 and Figure 16 in the Appendix.

1.2.5 Equilibrium Dialysis Experiments

Conditional distribution coefficients (K_D) of As-DOM complexation were determined through equilibrium dialysis adapted from Zhang et al. 2021. An illustration of equilibrium dialysis is shown in Figure 1. First, the pH of all solutions was adjusted to 7 ± 0.1 incrementally with 0.1 KOH and 0.1 HNO_3. For each DOM type, a DOM solution (25 mg/L C, 45 mL) was sealed inside of a dialysis tube (Spectra/Pro Biotech Cellulose Ester membrane, 200 Da MWCO) and immersed in 500 mL of 0.01 M NaCl solution in a 0.5 L high-density polyethylene bottle. The solution was stirred for 24 hours to achieve sodium-saturated DOM. Afterwards, the NaCl solution was removed and replaced by 500 mL of ultrapure water. After 24 hours, the ultrapure was removed and replaced with fresh ultrapure water. Arsenic standards were added to the dialysis tube to achieve concentrations of 0, 5, 10, 50, 100, 250, and 500 ppb As inside of the dialysis tube. The dialysis tubes were left submerged for 48 hours to reach equilibrium. Aliquots were removed separately from outside of the tube and inside for the tube for dissolved organic carbon and As concentration analysis. Dissolved organic carbon content and arsenic content analysis was performed by University of Georgia Laboratory of Environmental Analysis.

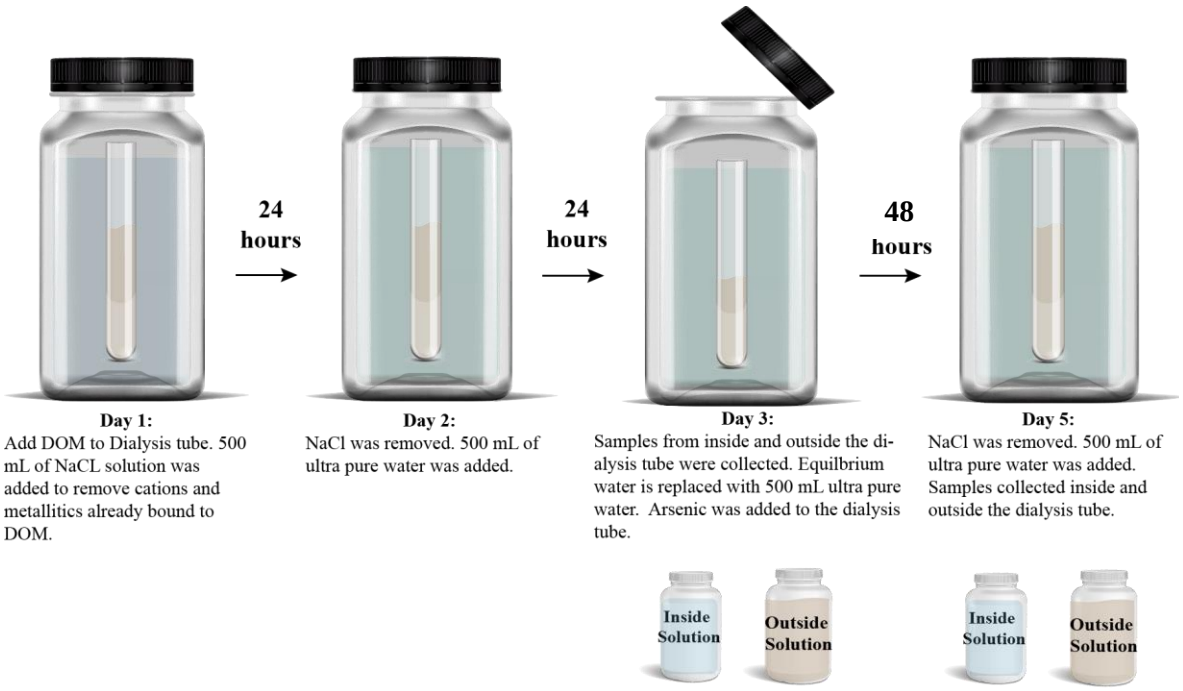

Figure 1: Illustration of equilibrium dialysis methodology

Conditional distribution coefficients (K_D) were calculated using the equation (EQ 3) from Buschmann et al., (2006) where $[As]_{s+w}$ represents As concentration inside the dialysis tube in µg L^{-1}, $[As]_w$ represents As concentration outside the dialysis tube in µg L^{-1}, [DOC] represents the total organic carbon concentration in kg L^{-1}, and [C] represents the carbon content in kg kg^{-1}. Carbon content of lignite derived DOM, reported in Ojeda et al., (2019), were 0.524 and 0.636 kg kg^{-1} for DH and HS respectively; carbon content for SRNOM, reported by the International Humic Substances society, was 0.507 kg kg^{-1}(International Humic Substance Society, 2022).

$$K_D = \frac{[As]_{s+w} - [As]_w}{[As]_w [DOC][C]} \qquad \text{(EQ 3)}$$

A mass balance, Table 4 in the Appendix, of the As and TOC content was performed to account for As and DOM in the experiments. The As mass balance was calculated using EQ 4 where $[As]_{background}$ represents the As concentration naturally found in the DOM source (µg), $[As]_{added}$ represents the theoretical As concentration added to the dialysis experiment, $[As]_{inside}$ represents the reported As concentration inside the dialysis tube (µg), and $[As]_{outside}$ represents the reported As concentration outside the dialysis tube (µg). The TOC mass balance was calculated using EQ 5 where $[TOC]_{background}$ represents the TOC concentration of the UPW (mg), $[TOC]_{added}$ represents the TOC concentration to dialysis tube (mg), $[TOC]_{inside}$ represents the reported TOC concentration inside the dialysis tube, and $[TOC]_{outside}$ represents the reported TOC concentration outside the dialysis tube (mg).

$$[As]_{background} + [As]_{added} = [As]_{inside} + [As]_{outside} \quad \text{(EQ 4)}$$

$$[TOC]_{background} + [TOC]_{added} = [TOC]_{inside} + [TOC]_{outside} \quad \text{(EQ 5)}$$

1.2.6 Free and Complexed As Determination through HPLC-SEC-ICP-MS

An inductively coupled plasma mass spectrometer (ICP-MS) (Agilent 7900 Quadrupole) was coupled to a high-performance liquid chromatography system (HPLC) (1200 HPLC Quaternary Pump, Agilent, USA) equipped with two size exclusion columns (SEC) (Protein-Pak 125, 10 µm, 7.8x300mm, Waters, USA) to form the HPLC-SEC-ICP-MS system. As-DOM samples (25mg/L C and 0, 5, 10, 50, 100, 250, and 500 ppb As) were analyzed for each DOM type. Ammonium nitrate (0.01 M) solution was used as mobile phase. The HPLC-SEC-ICP-MS system analyzed in no gas mode at flow rate of 1 mL/min for 40 minutes. The injection volume was 100 µL, and each sample was measured in duplicate.

As-DOM samples (25mg/L C and 0, 5, 10, 50, 100, 250, and 500 ppb As) were also analyzed a through HPLC-SEC with fluorescence (FLD) and ultraviolet (UV) detectors (HPLC-SEC-FLD/UV system). The HPLC-SEC-FLD/UV held a flow rate of 1 mL/min for 45 minutes with a sample injection volume of 50 µL. Excitation and emission wavelengths for the FLD detector were chosen individually for each DOM type from fluorescence excitation-emission matrices (EEMs) analyzed on a FP-8500 spectrofluorometer (JASCO, USA) described in Malina et al. (2022) (in preparation). The UV detector was set to an absorbance of 254 nm. Each sample was measured in duplicate.

1.3 Results

1.3.1 Equilibration Time

The equilibration time, used in previous research, is diverse ranging from two hours to two weeks (Bauer and Blodau, 2009; Ritter et al., 2006). A series of dialysis experiments, shown in Figure 1, were completed with the collection time ranging from 6 – 96 hours. Initially, there was a sharp change in the log K_D from 6.55 to 4.59 within the first 24 hours. Between 24-96 hours, the log K_D appears to stabilize between 3.86 and 4.16. The stabilization of the log K_D suggests that the system reached equilibrium at 24 hours validating the use of 24 hour minimum before analysis.

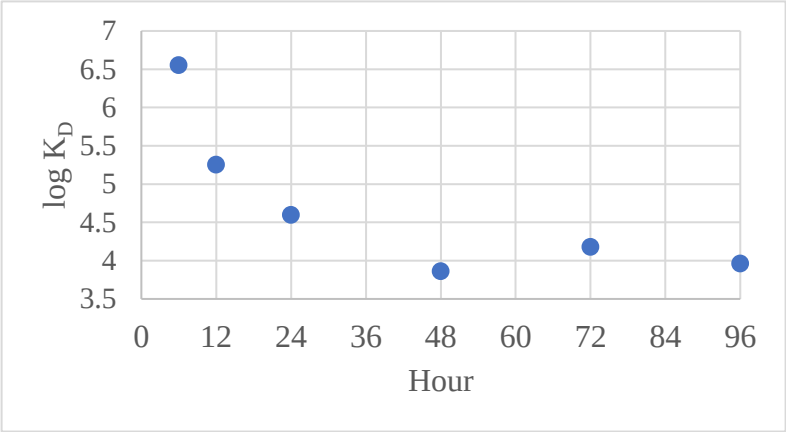

Figure 2: Comparison of log K_D from equilibrium dialysis with lignite derived DOM and treatment of 500 ppb As at a pH of 7 ±0.1. Samples were collected after 6, 12, 24, 48, 72, and 96 hours.

1.3.2 Detection of As-DOM Complexes through HPLC-SEC-ICP-MS Analysis

In size exclusion chromatography, the stationary phase can precisely separate compounds by molecular weight. In the stationary phase, larger compounds elute first while smaller compounds enter the pores of the column resulting in a longer pathway and larger retention time.

By coupling SEC with different detectors, we can directly match the absorbance, fluorescence, or mass-charge ratio properties to compounds of certain molecule weights.

The HPLC-SEC-ICP-MS system was used in separation and detection of free and complexed As, while HPLC-SEC-FLD and HPLC-SEC-UV was used to detect the fluorescence and absorbance properties of DOM compounds. HPLC-ICP-MS analysis has been used to determine the speciation of As, however, this technique was not recommended as a tool to detect As^{III}-DOM and As^{V}-DOM complexes simultaneously as they both have the same retention times (Liu and Cai, 2014). We did not expect As speciation throughout our experiment, using Geochemist Workbench, we determined that As would remain as As^{III} throughout our experiments. The overlapping HPLC-SEC-ICP-MS and HPLC-SEC-FLD chromatographs are shown in Figure 2-4 and the overlapping HPLC-SEC-ICP-MS and HPLC-SEC-UV VIS are shown in Figure 5-7.

Two peaks were observed from HPLC-SEC-ICP-MS analysis at approximately minute 17 and 28 in all As treatments and DOM types (Figures 2-4). In lignite derived DOM samples (DH and HS, Figures 2-3) an additional As peak was observed at minute 13. At approximately 17 minutes, there is observable As peak, from HPLC-SEC-ICP-MS system, and DOM peak, from HPLC-FLD, shown by the red line. The matching retention time of these peaks in both chromatographs is consistent with all As treatments and DOM types and suggests the detection of As-DOM complex.

There are three lines of evidence suggesting that the 28 minute peak represents free As. First, there lacks a corresponding DOM peak detected in the FLD or UV-Vis spectra, suggesting that the 28 minute peak is not an As-DOM complex. Second, free As, a smaller molecule, elutes later than complexed As which is in agreement with SEC theory. Finally, control samples of free As matched the respective retention time (28 minutes) (Figure 20 in the Appendix), however we

did notice a minor 17 minute peak in some samples that will a result of trace organic material in the UPW. The retention time for the 17 minute peak matches the As-DOM complex peak, however there was no evidence of organic material through FLD and UV analysis. We expect the poor response from FLD and UV analysis is likely caused by low concentration of DOM within UPW. The 28 minute peak also responded linearly to increasing concentrations of As (Figure 18 in the Appendix).

As complexation behavior changes with different treatments of As, denoted by the (A)-(F) symbol in Figures 2-4. At 0 ppb As, a background As concentration is observed but the majority of As is bound within the DOM fraction. With the smaller As treatments, e.g. 5-50 ppb, we can observe an equal increase in bound and free As. With larger As treatments, i.e. 100 and 500 ppb, the majority of As is free As, which could be caused by the saturation of As and loss of complexation sites within the DOM molecule.

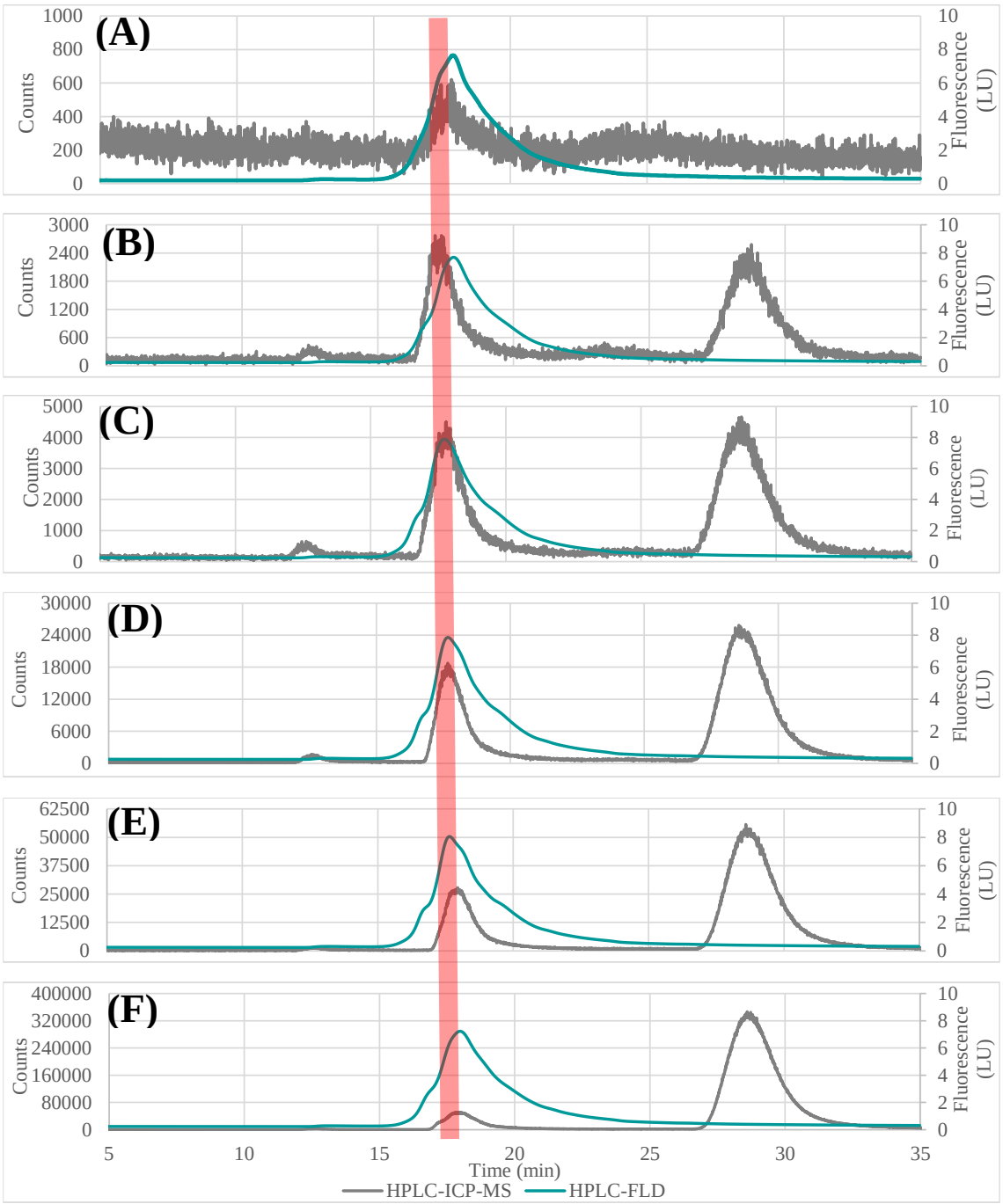

Figure 3: HPLC-SEC-ICP-MS (gray line, left y axis) and HPLC-SEC-FLD (green line, right y axis) chromatographs of As complexation with DH. The As treatment ranged from 0-500 ppb: 0 ppb (A), 5 ppb (B), 10 ppb (C), 50 ppb (D), 100 ppb (E), and 500 ppb (F)

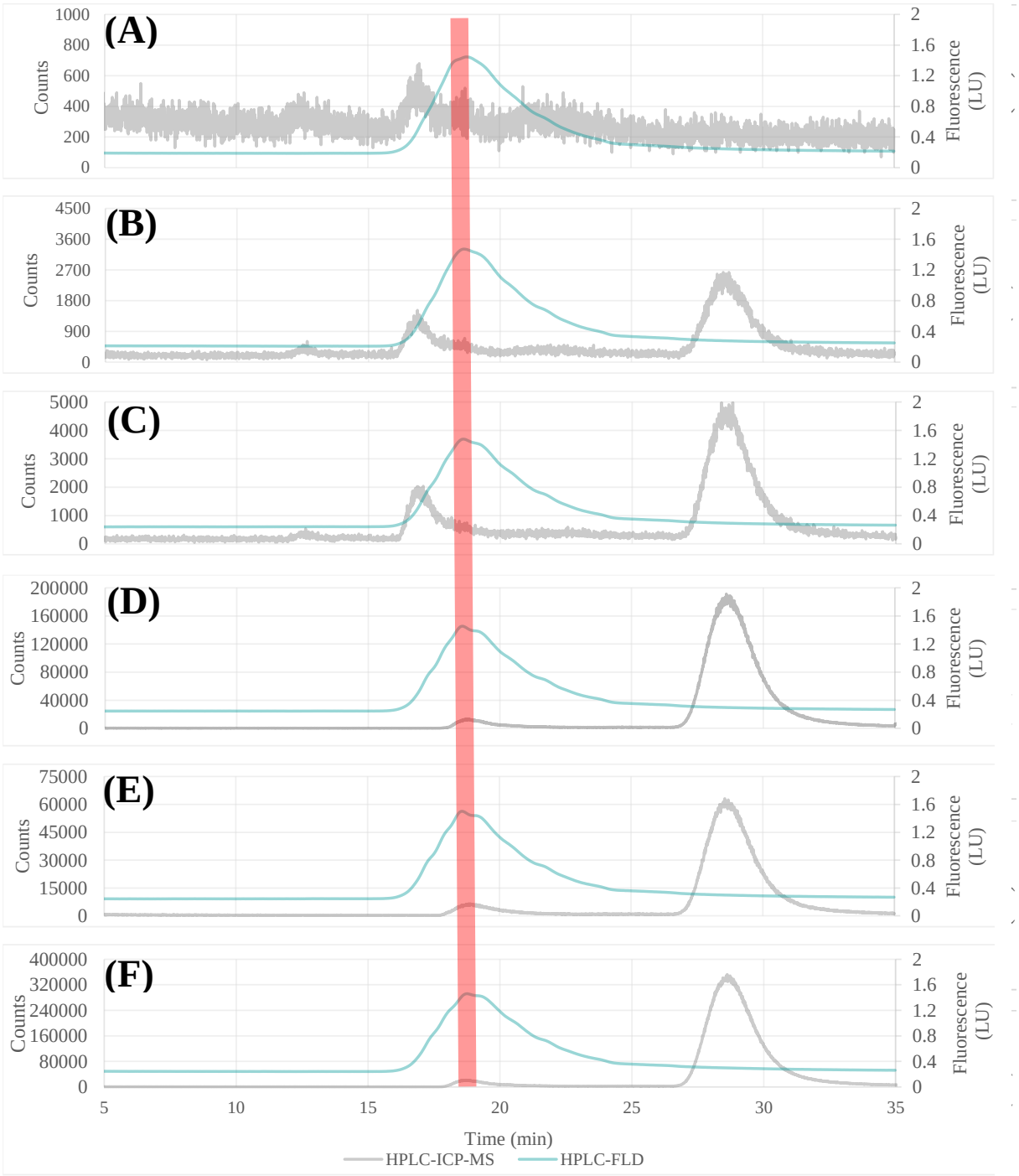

Figure 4: HPLC-SEC-ICP-MS (gray line, left y axis) and HPLC-SEC-FLD (green line, right y axis) chromatographs of As complexation with HS. The As treatment ranged from 0-500 ppb: 0 ppb (A), 5 ppb (B), 10 ppb (C), 50 ppb (D), 100 ppb (E), and 500 ppb (F)

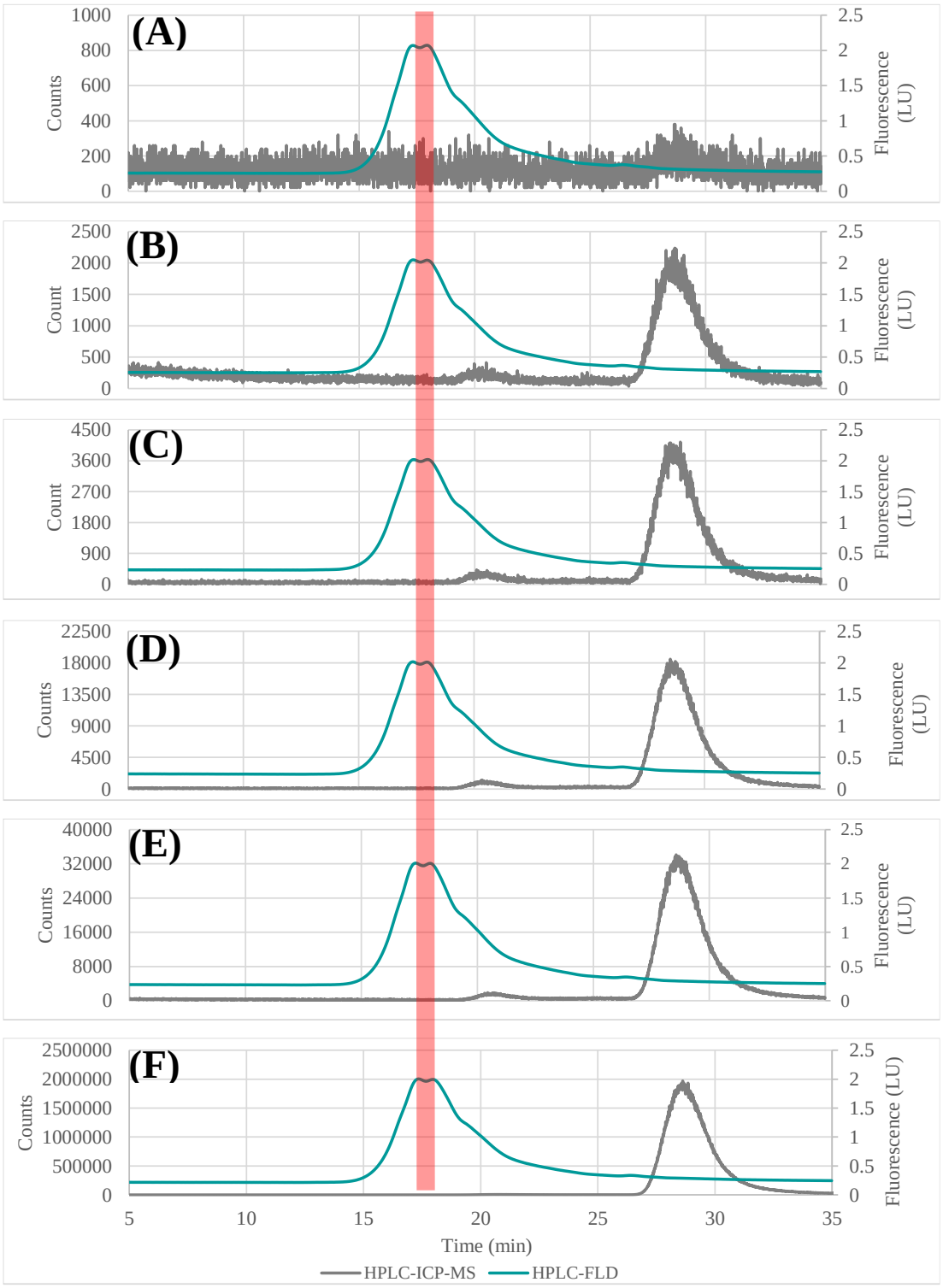

Figure 4: HPLC-SEC-ICP-MS (gray line, left y axis) and HPLC-SEC-FLD (green line, right y axis) chromatographs of As complexation with SRNOM. The As treatment ranged from 0-500 ppb: 0 ppb (A), 5 ppb (B), 10 ppb (C), 50 ppb (D), 100 ppb (E), and 500 ppb (F)

Consistent with the fluorescence chromatographs, the HPLC-SEC-UV system produced observable peaks at minute 17 and 13 (for the lignite derived DOM). Similar to the FLD chromatographs, there was no peak from the HPLC-SEC-UV system at minute 28. The lack of no UV-VIS peak at minute 28 is additional evidence that this peak represents the free As.

The similar retention time of peaks at minute 17 from the HPLC-SEC-UV and HPLC-SEC-ICP-MS systems is indicated by the red line. Overlapping peaks were observed within the 17-minute peak; overlapping peaks occur in instances of poor separation when multiple molecules coelute at the same time. DOM is not a homogeneous substance but an assortment of molecules with a range of molecular weights. As may preferentially bind one or more moieties of different molecular weights contained within the 17-minute peak.

HPLC-SEC-UV and HPLC-SEC-ICP-MS systems produce peaks at minute 13, shown by the blue line, suggest the detection of another As-DOM complex. Since this complex elutes earlier than the other As-DOM complex and only has absorbance properties, Figures 5-7, the As-DOM complex is likely to be a larger chromophore.

Liu et al., (2011) and Liu and Cai, (2014) have investigated the use of HPLC-SEC-ICP-MS for separating and detecting As-DOM complexes and free As. Liu et al., (2011) identified direct evidence of As-DOM and As-Fe-DOM complexes using HPLC-SEC-ICP-MS and HPLC-SEC-UV analysis. The objective of Liu and Cai, (2014) was to assess the precision and use of HPLC-SEC-ICP-MS and HPLC-SEC-UV analysis to detect DOM with different As species. Similar to our study, the similar retention time of peaks from HPLC-SEC-ICP-MS and HPLC-SEC-UV analysis was used as evidence of As-DOM complex. It must be highlighted that both studies employed Aldrich Humic Acid as the sole DOM type in these studies. Both studies did not observe overlapping peaks during UV analysis or the occurrence of more than one As-DOM

complex. However, the difference in results was likely caused from the authors sole reliance on Aldrich Humic Acid in their experiments.

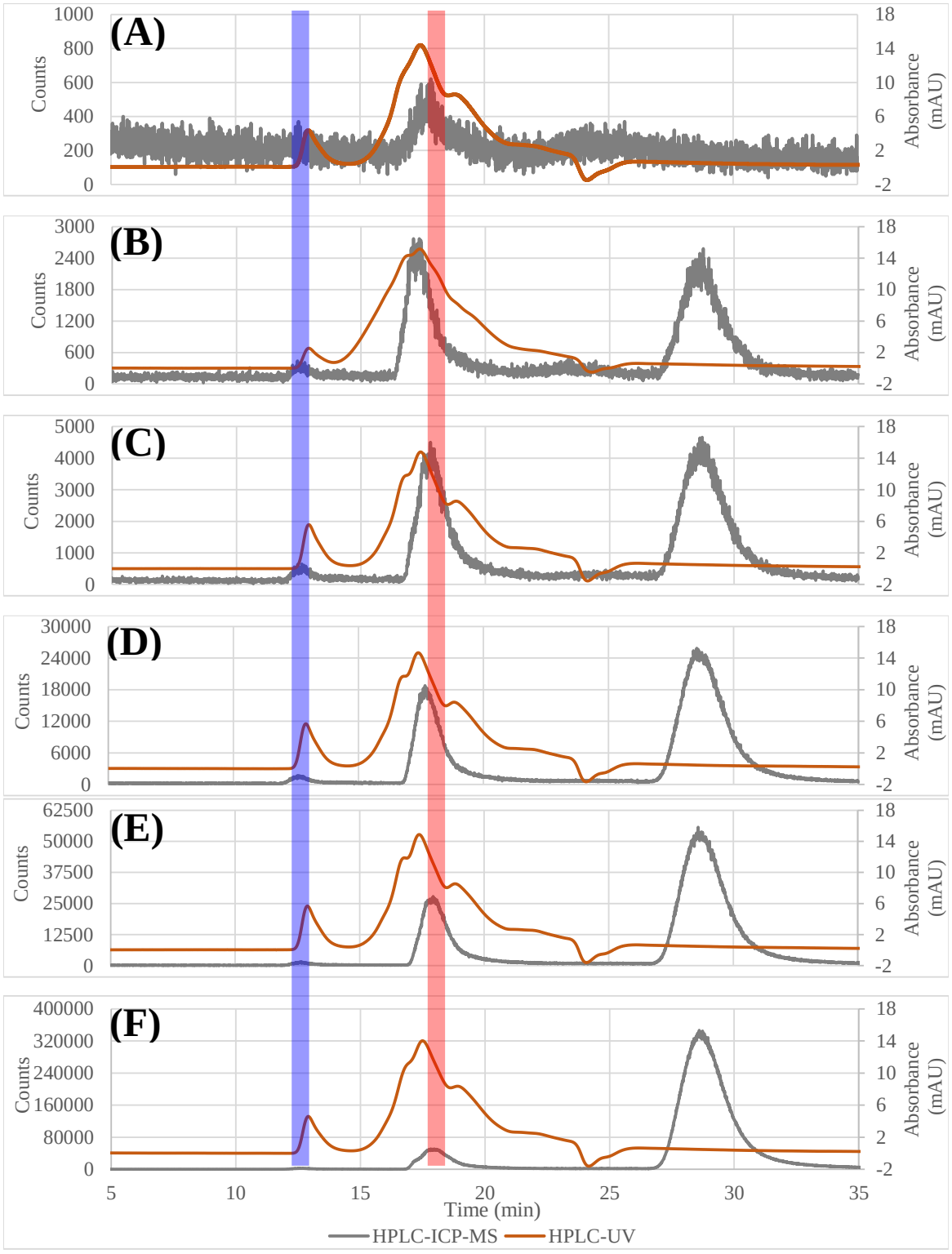

Figure 5: HPLC-SEC-ICP-MS (gray line, left y axis) and HPLC-SEC-UV (orange line, right y axis) chromatographs of As complexation with DH. The As treatment ranged from 0-500 ppb: 0 ppb (A), 5 ppb (B), 10 ppb (C), 50 ppb (D), 100 ppb (E), and 500 ppb (F)

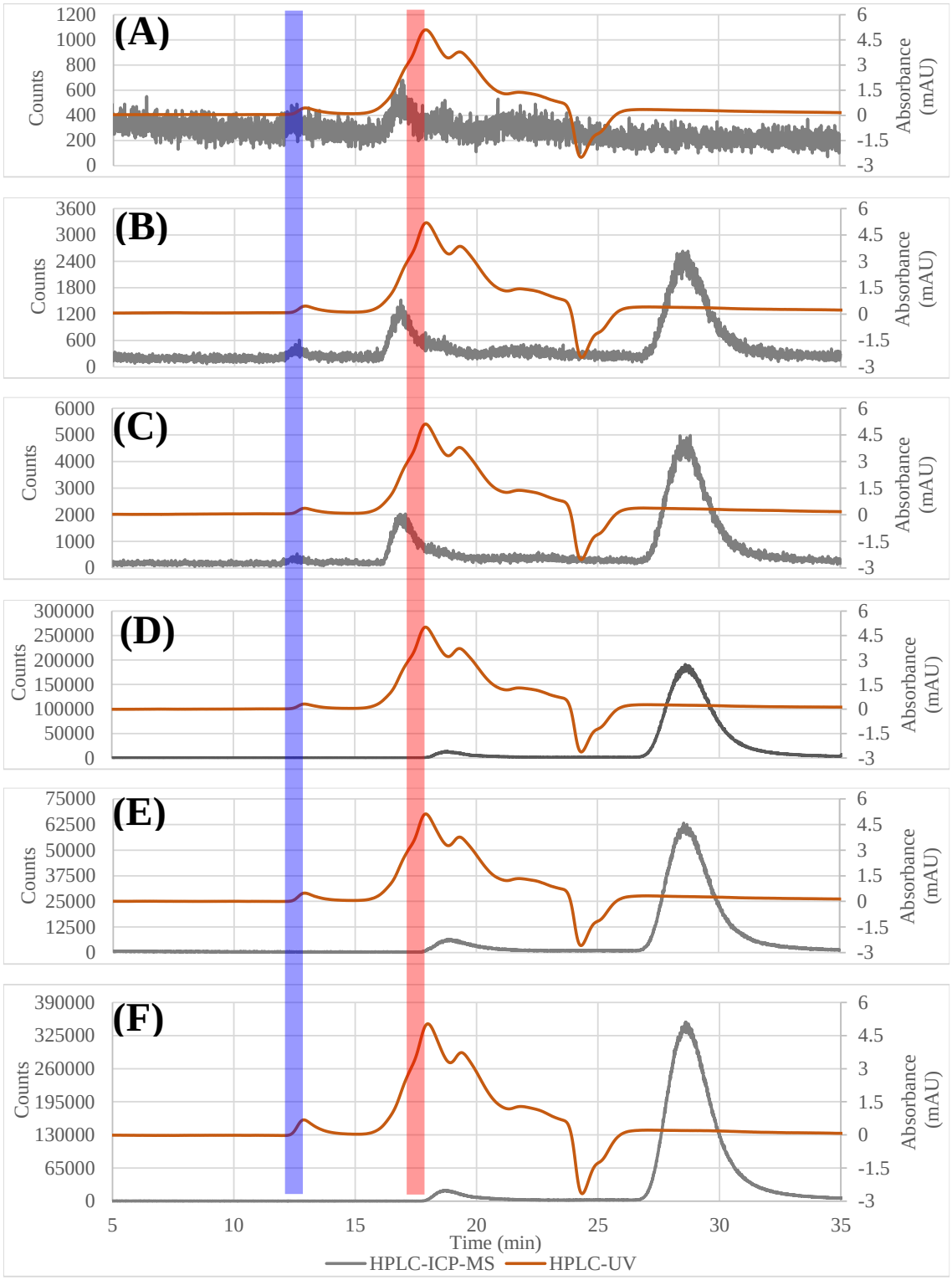

Figure 6: HPLC-SEC-ICP-MS (gray line, left y axis) and HPLC-SEC-UV (orange line, right y axis) chromatographs of As complexation with HS. The As treatment ranged from 0-500 ppb: 0 ppb (A), 5 ppb (B), 10 ppb (C), 50 ppb (D), 100 ppb (E), and 500 ppb (F)

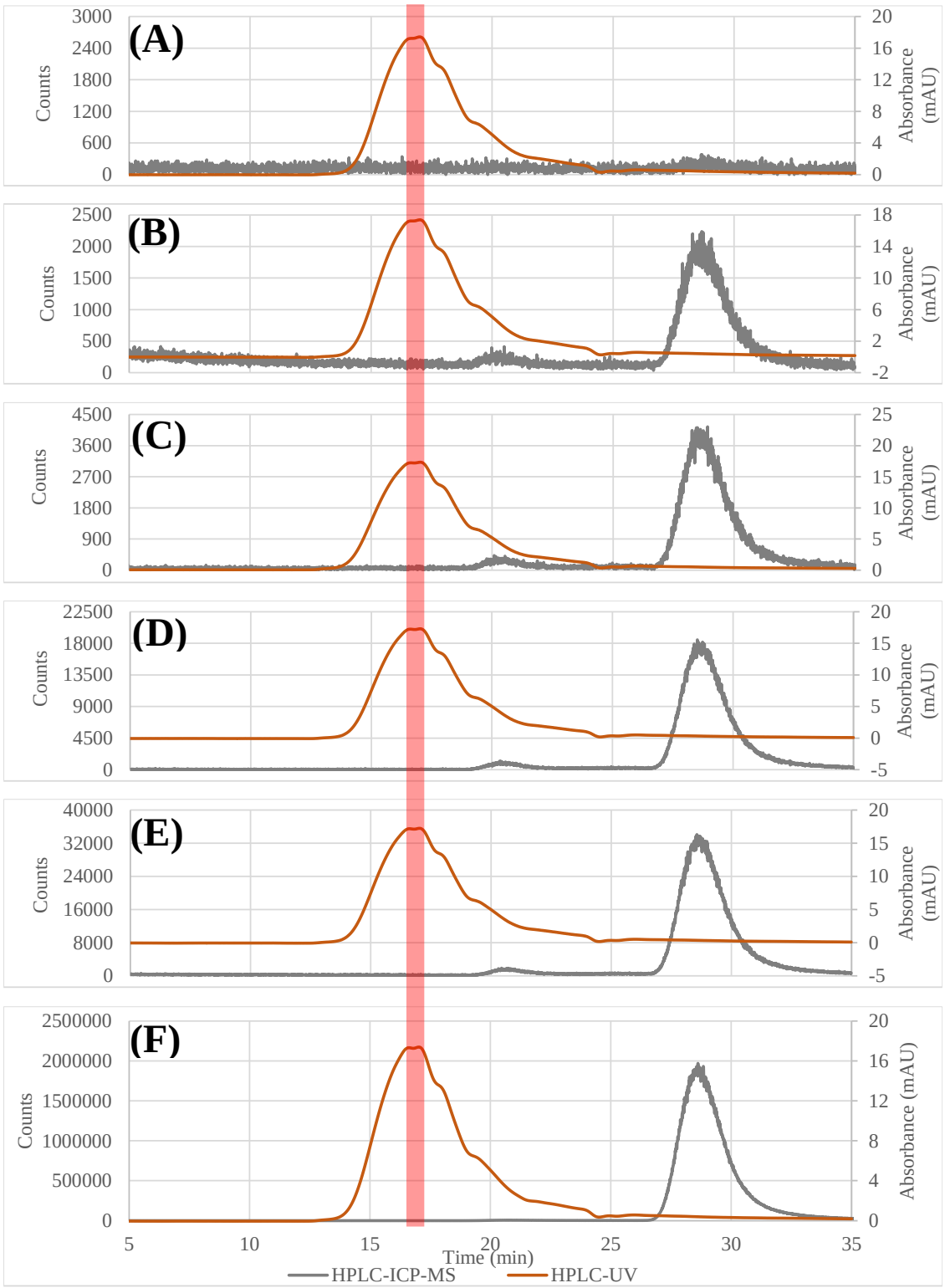

Figure 7: HPLC-SEC-ICP-MS (gray line, left y axis) and HPLC-SEC-UV (orange line, right y axis) chromatographs of As complexation with SRNOM. The As treatment ranged from 0-500 ppb: 0 ppb (A), 5 ppb (B), 10 ppb (C), 50 ppb (D), 100 ppb (E). and 500 ppb (F)

1.3.3 Detection of As-DOM through Equilibrium Dialysis

Dialysis is an indirect method of measuring As-DOM complexation. The molecular size distribution for the DOM used in our study ranged from 255-1308 Da, while the pore size of the dialysis tube was 500 Da. DOM movement is controlled by a semipermeable membrane of the dialysis tube while As has the ability to move freely. Equilibrium dialysis experiments results are illustrated in Figure 8.

Despite the As treatment, the majority of As was free As which is consistent with results from past dialysis experiments (Bauer and Blodau, 2009). The proportion of free As increased with larger As treatments. Similar to behavior exhibited in HPLC-ICPMS analysis, smaller As treatments exhibited higher proportion of As complexation than larger As treatments.

The SRNOM and HS experiments were highly variable, shown by the error bars in Figure 8B and C. However, error bars do not appear for DH lignite DOM (Figure 8A) because the experiment was performed once.

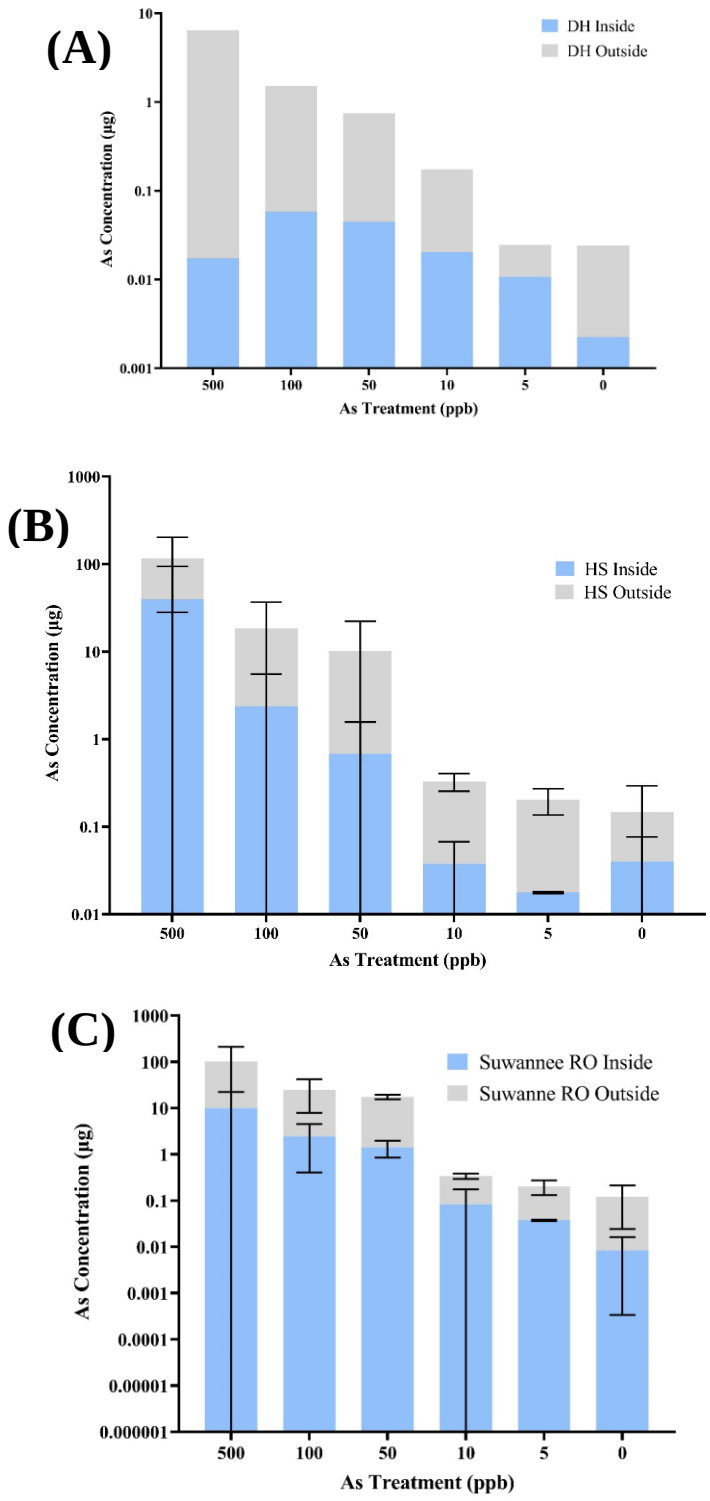

Figure 8: Equilibrium dialysis As measurements (µg, y axis) inside (blue) and outside (gray) of the dialysis tube. All three DOM types were used, Dolet Hills DOM (A), Hot Springs DOM (B), and Suwanne RO Humic Acid (C), with As treatments (ppb, x axis) of 500, 100, 50, 5, 0 at a pH of 7.0 ±0.1

1.3.4 Comparison of As-DOM Complexation

As-DOM conditional distribution coefficients (K_D) as a function of As concentration are shown in Figure 9. Log K_D values calculated from dialysis are represented by circles; log K_D calculated from HPLC-SEC-ICP-MS are represented by squares. In cases during HPLC-SEC-ICP-MS analysis when two complexation peaks were identified, the peak areas were added together to approximate the total complexation of those samples. Initially, log K_D values decreased with increased addition of As. The sharp decrease and overall pattern in K_D has been documented in Bauer and Blodau, (2009) and Liu and Cai, (2010). As previously discussed, the decrease in log K_D with the addition of As is likely caused by the oversaturation As and loss of complexation sites. There was no consistent pattern between DOM type and As complexation was identified across all analyses. However, log K_D values of lignite derived DOM (HS and DH DOM) from HPLC-SEC-ICP-MS analysis were higher than SRNOM values. Log K_D were consistently higher in dialysis experiments than those calculated from HPLC-SEC-ICP-MS analysis.

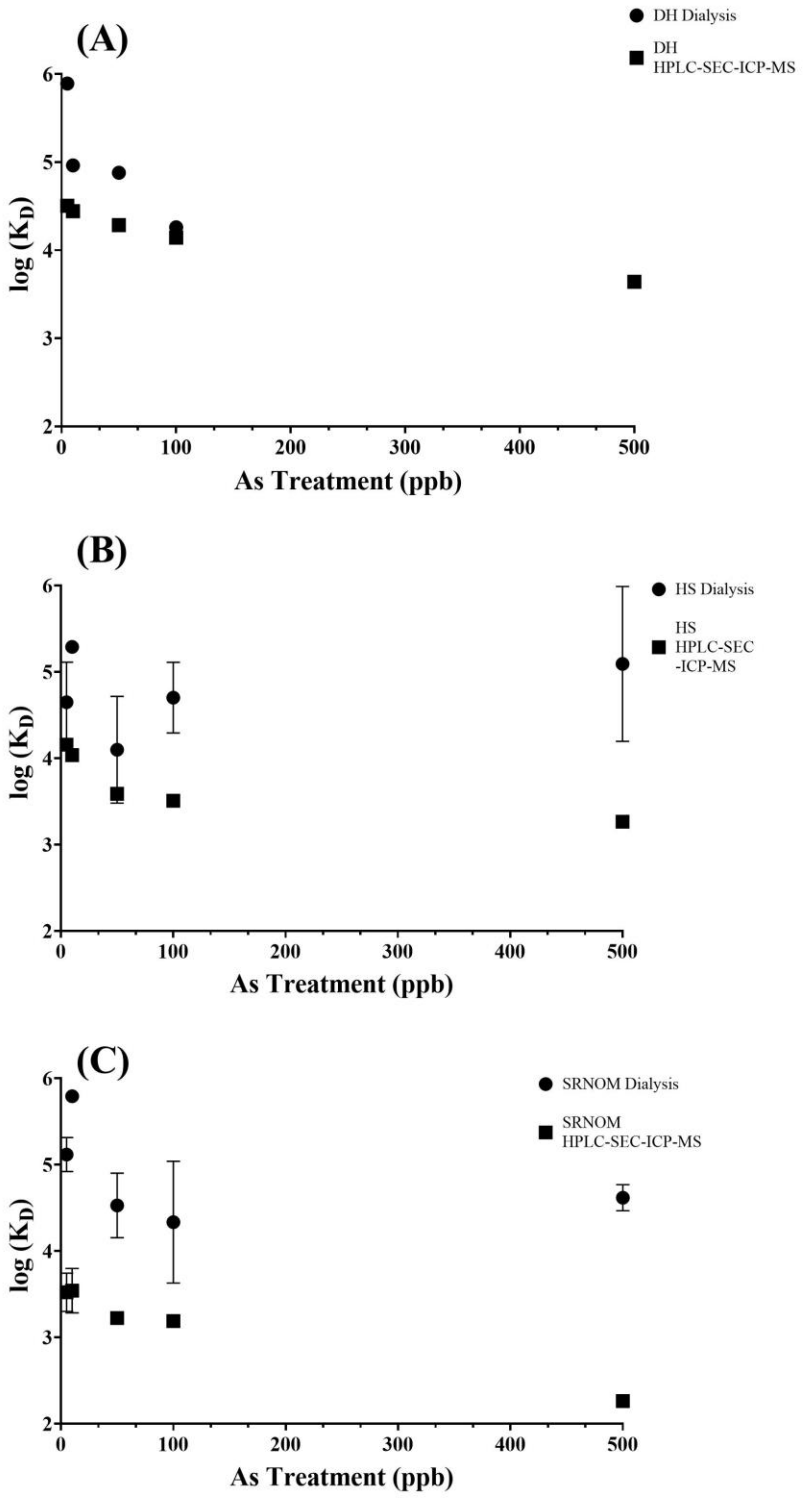

Figure 9: Conditional distribution coefficients (K_D) of As and DOM at a pH of 7.0 ±0.1. All three DOM types were used, DH (A), HS (B), and SRNOM (C), with As treatments (x axis) of 0, 5, 10, 50, 100, 500 ppb

The comparison of log K_D between this study and previous studies is exhibited in Table 1. The closest comparison are the HPLC-SEC-ICP-MS results of SRNOM from our study and Liu and Cai, 2010 with log K_D values ranging from 3.67-2.24 and 3.6–2.6 respectively. In general, log K_D values from our equilibrium dialysis experiments were higher than previous literature, specifically in Buschmann et al., (2006), however, the As treatments of previous literature are larger than the As treatments of this study. Most studies utilized an As treatment range that was an order of magnitude greater than this study's As treatment concentration, which make an evaluation between our study and previous study difficult to compare. Previous experiments exclusively utilized commercial DOM substances, Aldrich Humic Acid, with the exception of Buschmann et al., (2006). The chemical structures and properties of commercial DOM substances have been found to be dissimilar to natural occurring DOM substances; the difference is so pronounced that commercial DOM substances are not recommended as a substitution for natural DOM substances (Malcolm and MacCarthy, 1986). The differences in log K_D values may be a result of differences in experimental design including (1) reliance on commercial DOM, Aldrich Humic Acid and (2) use of higher concentration of As for treatments. There has been a lack of reporting of log K_D and K_D values in previous literature that is necessary to further investigate and validate novel methods of determining As-DOM complexes

Table 1: Comparison of conditional distribution coefficients, KD, of this study and previous literature.

Reference	Analysis	DOM	K_D	log K_D	pH	As (III) (ppb)	TOC (mg/L)
This study	Dialysis	SRNOM	619694-3348	5.79-3.52	7.0 ±.0.1	5-500	25
This study	Dialysis	Lignite-derived DOM (DH)	782443-18237	5.89-4.26	7.0 ±.0.1	5-500	25
This study	Dialysis	Lignite-derived DOM (HS)	532252-4577	5.72-3.66	7.0 ±.0.1	5-500	25
This study	HPLC-SEC-ICP-MS	SRNOM	5290-174	3.67-2.24	7.0 ±.0.1	5-500	25
This study	HPLC-SEC-ICP-MS	Lignite-derived DOM (DH)	32047-4380	4.51-3.64	7.0 ±.0.1	5-500	25
This study	HPLC-SEC-ICP-MS	Lignite-derived DOM (HS)	14481-1842	4.16-3.26	7.0 ±.0.1	5-500	25
Buschman et al. 2006	Dialysis	Suwanee River Humic Acid	540	1.58	6.2	750	4.0 nmol mg $_{DOC}^{-1}$
Liu and Cai	HLPC-SEC-ICP-MS	Aldrich Humic Acid	3981-398	3.6-2.6	7.0 ±.0.1	5-5000	14
Fakour and Lin 2014	HPLC-HG-OES HPLC-HG-AFS	Aldrich Humic Acid	13000-2000*	4.1-3.3*	7.5	200-4000	30
Fakour and Lin 2014	HPLC-HG-OES HPLC-HG-AFS	Aldrich Humic Acid	8500-1500*	3.9-3.2*	7.5	200-4000	15
Fakour and Lin 2014	HPLC-HG-OES HPLC-HG-AFS	Aldrich Humic Acid	6500-1000*	3.8-3.0*	7.5	200-4000	5
Fakour and Lin 2014	HPLC-HG-OES HPLC-HG-AFS	Aldrich Fulvic Acid	4500-1000*	3.7-3.0*	7.5	200-4000	30

*Estimated data from figures reported in previous literature.

1.3.4 The Changes of Optical Properties with Complexation

Spectroscopic methods have been utilized as tools to investigate responses of the chromophores and fluorophores in the presence of metals (Li and Hur, 2017). DOM is comprised of chromophores and fluorophores which are portions of the molecule that are responsible for absorption or fluorescence properties respectively. These properties are highly sensitive to environmental changes and complexation reactions (Tipping, 2002). The metal-DOM can alter spectroscopic properties by quenching or amplifying the fluorescence and/or absorbance of DOM peaks in the presence of a certain metal (Li and Hur, 2017).

In this study, molar absorptivity values, shown in Figure 10, were calculated to evaluate the influence of As on absorption measurements. Molar absorptivity determines the strength of DOM absorption properties. Beer's law (EQ. 2) states that absorption is proportion related to concentration and molar absorptivity of a substance. Changes in molar absorptivity can alter results when either quenching or enhancing of absorbance during HPLC-SEC-UV VIS analysis. Seven different As treatments, 0, 5, 10, 50, 100, 250, 500 ppb, and four wavelengths, 254, 280, 350, and 400 nm, were investigated. The lignite derived DOM, in (A) and (B), showed no changes in molar absorptivity across all wavelengths and As treatments. SRNOM, shown in subfigure (C), indicated a sharp drop in molar absorptivity between 0 and 5 ppb As treatments. However, there appeared to be no change in the molar absorptivity values in the other As treatments. We can conclude that As addition had no observable impact on the absorption properties of DOM throughout our experiments.

Differential spectra, the difference between an original spectra and an altered spectra, has been employed to examine DOM reactivity (Li and Hur, 2017). DOC normalized spectra has been used to identify chromophores responsible for complexation in Zhang et al., 2021. A compressed

DOC normalized differential spectra for all treatments and DOM types is shown in Figure 11. Chromophores are identified by consistent quenching or enhancing of a portion of the DOC normalized differential spectra. No consistent quenching or enhancing was observed across all DOM types.

SRNOM showed one potential chromophore at 235 nm. With the addition of As, there was a consistent decrease in the DOC normalized differential spectra until 100 ppb As. There was no difference in the spectra when comparing SRNOM 100 ppb As, 250 ppb As, and 500 ppb. These results are inconsistent with Zhang et al., (2021) who saw a consistent increase in their spectra with the addition of As and As-active chromophores in the 100 and 210 nm range.

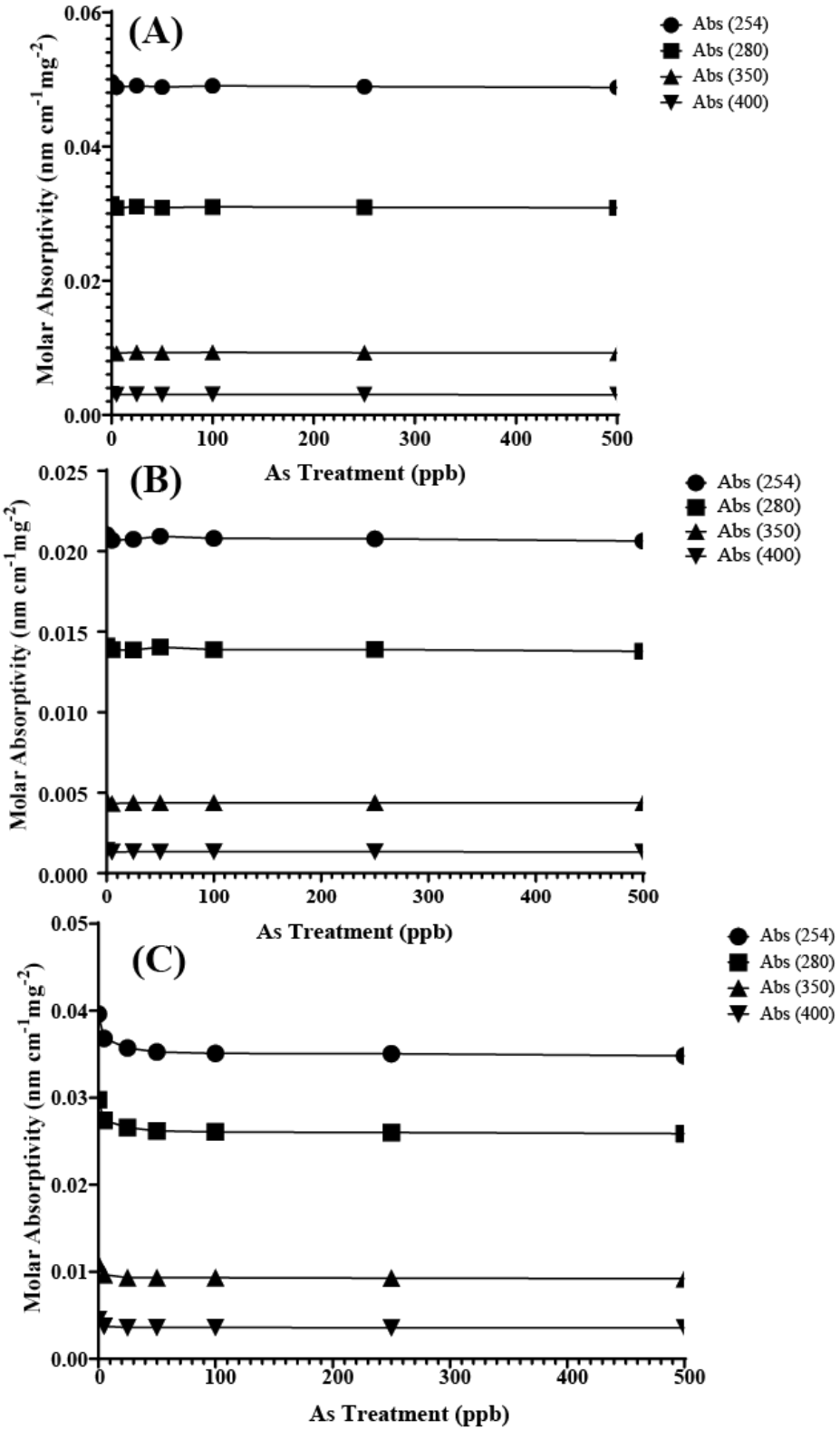

Figure 10: Molar Absorptivity of DOM at wavelengths of 254 (circle), 280 (square), 350 (star), and 400 (triangle) nm. All three DOM types were used, DH (A), HS (B), and SRNOM (C), with As treatments (x axis) of 0, 5, 10, 50, 100, 500 ppb

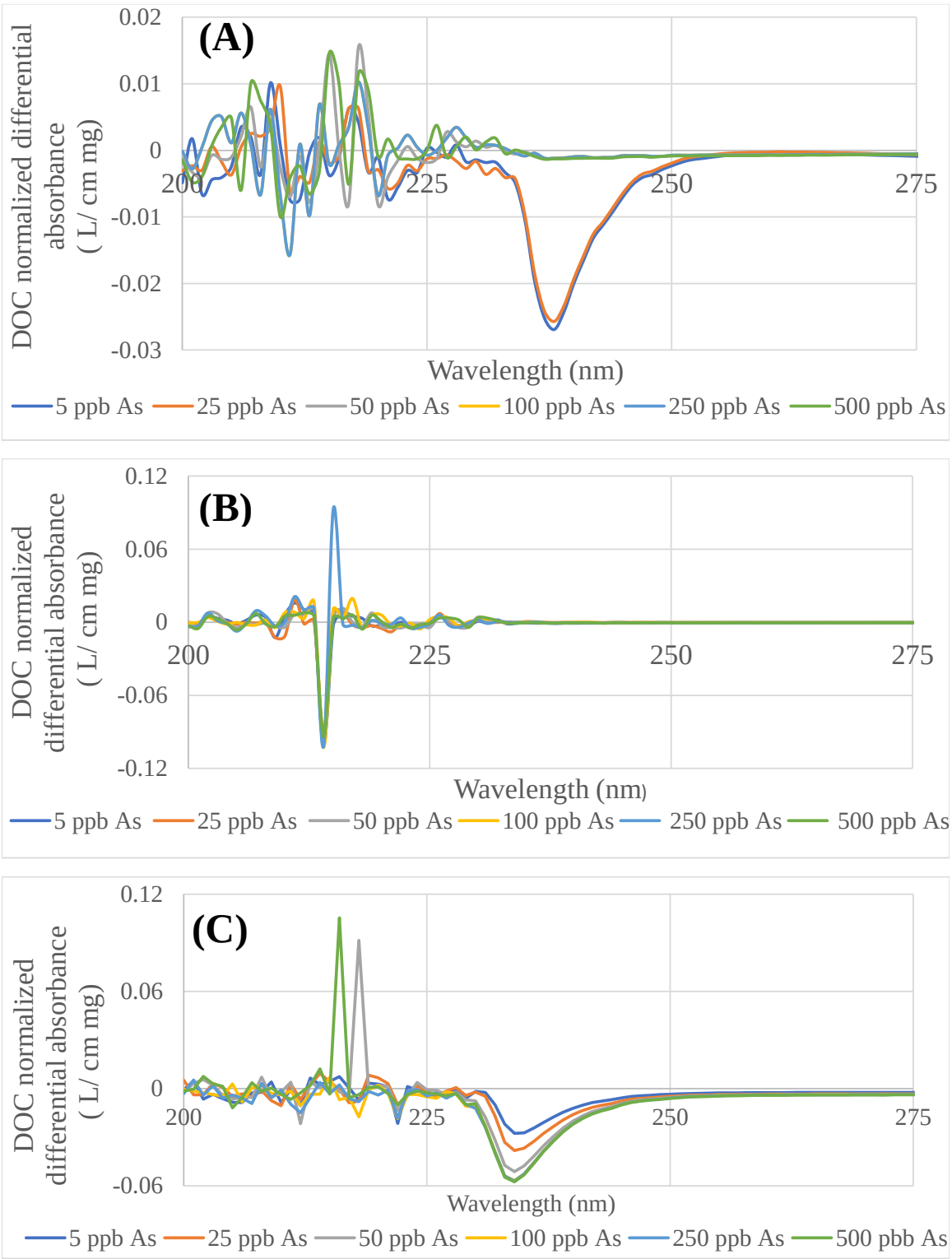

Figure 11: DOC normalized differential absorbance of DOM at a pH of 7.0 ±0.1 with As treatments of 5, 25, 50, 100, 250, and 500 ppb. All three DOM types, DH (A), HS (B), and SRNOM (C), were used and standardized to 25 mg/L

1.3 Discussion

1.3.1 Relationships between DOM Properties and Complexation

The detection of two As-DOM complexes of different molecular weights, as shown in Figures 5, 6, and 7, raise important questions on the impact of molecular weight on complexation. In lignite derive DOM samples, the formation of a larger molecular weight As-DOM complex (13-minute As-DOM complex) occurred across almost all As treatments. Our initial thoughts for this occurrence was that the lignite derived DOMs had a larger molecular weight moieties than SRNOM to form the larger molecular weight As-DOM complex. The molecular weights and size distributions of the DOM used in this study are listed in Table 2. SRNOM has a largest average molecular weight with similar size distribution to the lignite derived DOMs. The evidence of a larger molecular weight does not support this line of thought, therefore suggesting that the larger moieties of lignite derived DOM may have different chemical properties and that complexation is not dependent on molecular weight alone.

Two studies have investigated the impact of molecular weight on metal-DOM complexation. Ren et al., (2017) identified no relationship between hydraulic diameter and As-DOM complexation. Tadini and Moreira, (2014) found that DOM with a molecular size of < 10 kDa and 10-30 kDa had the highest binding capacity between DOM and chromium. The molecular weights of all DOM used throughout this study are significantly smaller than the molecular cutoffs used by both studies. Additional analysis is required to identify chemical or physical properties responsible for increased binding capacity in lignite derived DOM.

Table 2: Molecular Weights of DOM standards used in this study completed in Malina et al. 2022 (in preparation)			
DOM Type	Weight Averaged Molecular Weight (Da)	Number Average Molecular Weight (Da)	Size Distributions (Da)
Lignite Derived DOM (DH)	1172.5	1010.7	341-1471
Lignite Derived DOM (HS)	1251.6	1018.5	255-1042
SRNOM	2004.2	1429.7	534-1308

Two mechanisms have been determined to responsible for As-DOM complexation; these mechanisms include As, as a hydroxo complex, (1) creating an ether through ligand exchange reactions with a phenolic hydroxyl group and (2) creating an adduct with a carboxylate group (Ren et al., 2017). Positive relationships have been found between complexation and phenolic functional groups, carboxylic functional groups, and total acidity, the sum of phenolic and carboxylic functional group content (Ren et al., 2017). However, there were no differences in the phenolic and carboxylic functional group content between the three types of DOM used in our study, shown in Table 3 in the Appendix, that could then justify different K_D values.

Despite the addition of As, SRNOM has the higher $SUVA_{254}$ responses, shown in Figure 17 in the Appendix, than the lignite derived DOM. Higher $SUVA_{254}$ values, proxy indicator of aromaticity, have been used to suggested to be linked to reactivity (Weishaar et al., 2003). Our results did not produce any evidence of a relationship between complexation capacity and increased $SUVA_{254}$ responses or functional group content therefore suggesting that there are different mechanisms or properties are responsible for the complexation capacity.

The lower complexation capacity in SRNOM may be a response to lower background concentrations of iron (Fe) compared to those found in lignite derived DOM. Fe can facilitate the formation of a ternary complex through a Fe bridge or an (oxy)hydroxide surface complexation

Fe has been documented to have a significant effect on As-DOM complexation (Bauer and Blodau, 2009; Li et al., 2019; Liu et al., 2011; Ritter et al., 2006). Ritter et al., (2006) identified a statistically significant linear relationship between Fe content and complexed As concentration. Liu et al., (2011) produced direct evidence of the formation of As-Fe-DOM complex through HPLC-SEC-ICP-MS and HPLC-SEC-UV analysis. Background concentrations of Fe were higher in lignite derived DOM; concentrations were reported in Ojeda et al., 2019 and Malina et al., 2022 with concentrations of 6.7, 7.9, and 0.2 ppm for DH, HS, SRNOM respectively. We hypothesize that the higher concentration of Fe increased the complexation capacity of lignite derived DOM as lignite derived DOM are more likely to form both ternary As-Fe-DOM complex and As-DOM complex.

However, the suggestion of Fe as the primary cation facilitating the formation of ternary complex is based on the limited literature. A large gap in knowledge remains regarding the formation of ternary complexes, their stability, and empirical evidence of metals acting as bridges between As and DOM. Calcium (Ca), magnesium (Mg), aluminum (Al), and manganese (Mn) have been identified as metals that participate in bridging As to DOM (Lin et al., 2004; Redman et al., 2002). The binding mechanisms of these additional metals have not been identified; additional analysis is required to understand the precise mechanisms responsible is warranted.

1.3.2 Comparison of Methodology for Determining As-DOM Complexation

Our results were comparable to past studies, Table 1, and across both analysis methods, Figure 9. The precision of HPLC-SEC-ICPMS and dialysis were evaluated by analyzing As in ultrapure water of similar treatments. The calibration curve, shown in Figure 18 in the Appendix, and additional information, Table 5, produces reproducible precise results (R^2 =0.9612). Results from

the HPLC-SEC-ICP-MS systems consistently produced smaller K_D values than equilibrium dialysis despite DOM type or treatment.

As-DOM complex detection by equilibrium dialysis presents multiple limitations that hinder the accuracy of the results due to systematic error propagated by the methodology. Equilibrium dialysis methodology produced higher variation in the results, shown in Figure 9, compared to HPLC-SEC-ICPMS analysis. Documented errors from equilibrium dialysis methodology include (1) Gibbs-Donnan equilibrium effects, a phenomenon occurring when an impermeable barrier limits chemical equilibrium and produces an electrochemical gradient, (2) adsorption to the dialysis membranes (3) contamination from the dialysis membrane (Desoye, 1988). These have not been systematically explored in the literature and were not addressed in this work. Despite a poor mass balance, the K_D values for SRNOM were comparable to previous literature.

When HPLC-SEC-ICPMS results are analyzed in tandem with FLD and UV detectors, three lines of evidence of As-DOM complexes are produced. This technique appears to be more precise and requires fewer resources and time. Additionally, this is the first study to directly identify two separate As-DOM complexes. Importantly, inferential techniques like dialysis would not have been able to detect separate and measure these complexes. Therefore, the HPLC-SEC-ICPMS technique provided new insights to As-DOM complexation.

1.3.3 Limitations

All experiments were conducted under low ionic strength, oxic conditions, low light, and neutral pH conditions. The formation of As-DOM is highly sensitive to changes to environmental conditions. Although the conditions utilized are best to understand the general mechanisms governing complexation; our results cannot be extrapolated to all environmental systems. Additionally, it may not be possible to investigate changes in environmental conditions listed

above because many of the variables are dictated by the HPLC-SEC-ICPMS operating conditions. For example, the pH, redox conditions, and ionic strength are all dictated by the mobile phase, which would propagate changes to the instrument itself or the methods before these factors could be explored.

Although an improvement from past literature, which rely exclusively on commercial DOM, this study utilized only one DOM standard and two unique DOM types. With varied response from all three types of DOM, it is crucial to begin to investigate a more diverse pool of DOM sources to best extend literature to environmental systems. We advise future studies to investigate complexation with diverse types of DOM standards in order to make accurate predictions of As mobility in different systems. Equilibrium dialysis techniques requires a lengthy time commitment and a considerable number of resources both of which became limited throughout this study; consequently, the number of replicates in this study were severely limited.

Finally, few studies have reported the mass balance to evaluate the precision of equilibrium dialysis methodologies. There has been little evidence of mass balances completed by previous literature with the exception of Ritter et al., (2006). Additionally, many studies do not report K_D values associated with the study, therefore fit is difficult to compare results across these studies with dissimilar As treatments, environmental conditions, and analysis methods.

1.3.4 Environmental Impact

As previously stated, this is the first study to investigate As-DOM complexation with groundwater-based DOM. HPLC-SEC-ICP-MS analysis revealed that lignite-derived DOM K_D values were higher the Suwannee standard. Higher K_D values suggest groundwater DOM have a higher complexation capacity for As compared to the standard. The higher complexation capacity produces a potential gap in knowledge when references past modeling literature. Groundwater

DOM may be acting as a larger sink of As than predicted by previous literature. Additional research is required to understand if higher complexation capacity is a trait of all groundwater DOM or only the lignite derived DOM used in this study.

1.3.5 Future Directions.

HPLC-SEC-ICP-MS system analysis presents the opportunity to analyze As-DOM complexes directly in environmental samples. Environmental samples are subjected to conditions more complex than those predicted through laboratory modeling. Analysis of the environmental samples in tandem with laboratory modeling will highlight the relatability of laboratory predictions and additional factors controlling As cycling in the environment.

Due to time constraints, we were unable to investigate the influence of environmental conditions on As-DOM complexation. Environmental conditions alter the physiochemical characteristics of DOM thereby controlling the binding capacity of DOM and stability of As-DOM complexes (Liu et al., 2011). Lower molecular weight DOM substances, including fulvic acids, have a larger pH solubility ranges than higher molecular weighted DOM substances which would have a profound impact on their ability to engage in complexation reactions (Sharma and Sohn, 2009). Few studies have investigated the influence of environmental conditions. however there have been no studies that have coupled different environmental conditions with direct methods of determining As-DOM complexes. The environmental conditions of groundwater, high ionic strength, low oxygen content, and reducing conditions, have been typically ignored in studies investigating environmental conditions; this gap in knowledge needs to be filled to extend this research to groundwater systems.

Analysis of $SUVA_{254}$ and functional group content did not provide conclusive evidence of chemical properties associated with complexation. Carbon-13 nuclear magnetic resonance

spectroscopy (^{13}C NMR) and Fourier-transform infrared spectroscopy (FTIR) are analytical techniques that should be completed in collaboration with this study as these methods would provide evidence regarding precise mechanisms responsible for complexation.

1.4 Conclusion

This study confirmed the use of HPLC-SEC-ICPMS as a precise tool for determining As-DOM complexes; we recommend that future studies focus on the use of HPLC-SEC-ICPMS to gather more detailed information regarding the molecular characteristics of DOM fraction responsible for complexation. HPLC-SEC-ICPMS analysis suggests that lignite derived DOM has a larger complexation capacity compared to the literature standard, SRNOM, implying that complexation may be underestimated in groundwater systems in previous literature.

Chapter 2: Investigation of Coal Combustion Residuals Contamination in Alabama: A Coosa River Example

2.1 Introduction

Coal Combustion Residuals, CCR, are produced as a byproduct of coal-based electricity production (Wang et al., 2020). As one of the largest sources for electricity production, coal is responsible for over 40% of all electricity production in the US (American Road & Transportation Builders Association, 2015). CCR production has increased annually by 1.7 % since 1974 reaching 102 million tons in 2018. (American Coal Ash Association, 2018; American Road & Transportation Builders Association, 2015). CCR is stored in large quantities in coal ash pods, impoundments, and monoliths throughout the country (American Coal Ash Association, 2018). Over 600 surface impoundments have been identified throughout the US with 44 within the state of Alabama ("Coal Ash Issues in Alabama," 2014, "Effort to Assess Coal Combustion Residuals (CCR) Disposal Units," 2022).

In 2008, a CCR containment structure at the Kingston Power plant broke spilling 3.7 million cubic meters of CCR into the nearby watershed, which was one of the largest and most costly spills of CCR (Lemly and Skorupa, 2013). However, CCR contamination events are not limited containment breaches like the Kingston spill. Evidence of surface and subsurface leaking or flooding of CCR impoundments has been identified across the southeastern United States (Harkness et al., 2016; Vengosh et al., 2019). CCR contamination can have lasting environmental impacts on ecosystems and human health by contaminating soil, leaching into groundwater supply, or transporting into freshwater systems through run off or flooding events (Aguirre, 2019; Vengosh et al., 2019; Wang et al., 2020). CCR leachate is enriched in heavy metals which can impact ecosystems through bioaccumulation and biomagnification processes (Lemly and Skorupa, 2013;

Wang et al., 2020). In the last 45 years, the cost of CCR poisonings on ecosystems in the U.S. surpasses $2.3 billion; this cost is predicted to increase by another $3.85 over the next 50 years (Lemly and Skorupa, 2013).

Heavy metals from CCR can be preserved in aquatic sediments through sorption to suspended particles or oxyhydroxides in the water column and bottom sediments (Ruhl et al. 2012). The preservation and enrichment of heavy metals in sediment and water has been used as evidence of CCR contamination (Vengosh et al., 2019). A pattern of enrichment of trace elements As, Se, Cr, Hg, Ni, Co, Zn, Cu, Cd, Pb, Mo, Tl, Sb, V, Rh, and Fe can indicate CCR impacted sediment (Vengosh et al., 2019; Wang et al., 2020). Other diagnostic signatures of CCR contamination include low-field magnetic susceptibility, strontium or lead isotope fingerprint, and the presence of CCR particles (Aguirre, 2019; Brown et al., 2011; Harkness et al., 2016; Ruhl et al., 2012; Vengosh et al., 2019; Wang et al., 2020)

There are several CCR impoundments facilities in the Southeast USA, and nine within Alabama (Sackett, 2015). However, the impact of CCR on surface water and river sediment has not been reported in the literature. We hypothesize that CCR contamination will result in an enrichment of heavy metals in the sediment and surface water adjacent to CCR impoundments if there is contamination from groundwater discharge or flood events.

2.2 Materials and Methods

2.2.1 Study Site

This study focuses on the Coosa River which has two electricity generation plants, Ernest C. Gaston Electric Generating Plant and Gadsden Power Station, shown in Figure 2. Both plants have been operated by Alabama Power for over 60 years ("CCR Rule Compliance Data and Information," 2022). Potentiometric surface contour maps, completed by Alabama Power, suggest

some groundwater flow towards the Coosa River (Southern Company Services Earth Science and Environmental Engineering, 2022, 2019). By Gadsden impoundment facility, the Coosa flowed from the most upstream site, site 7, southwest to site 1 while at the Gaston impoundment, the Coosa flowed the most upstream site, site 14, southwest to site 8.

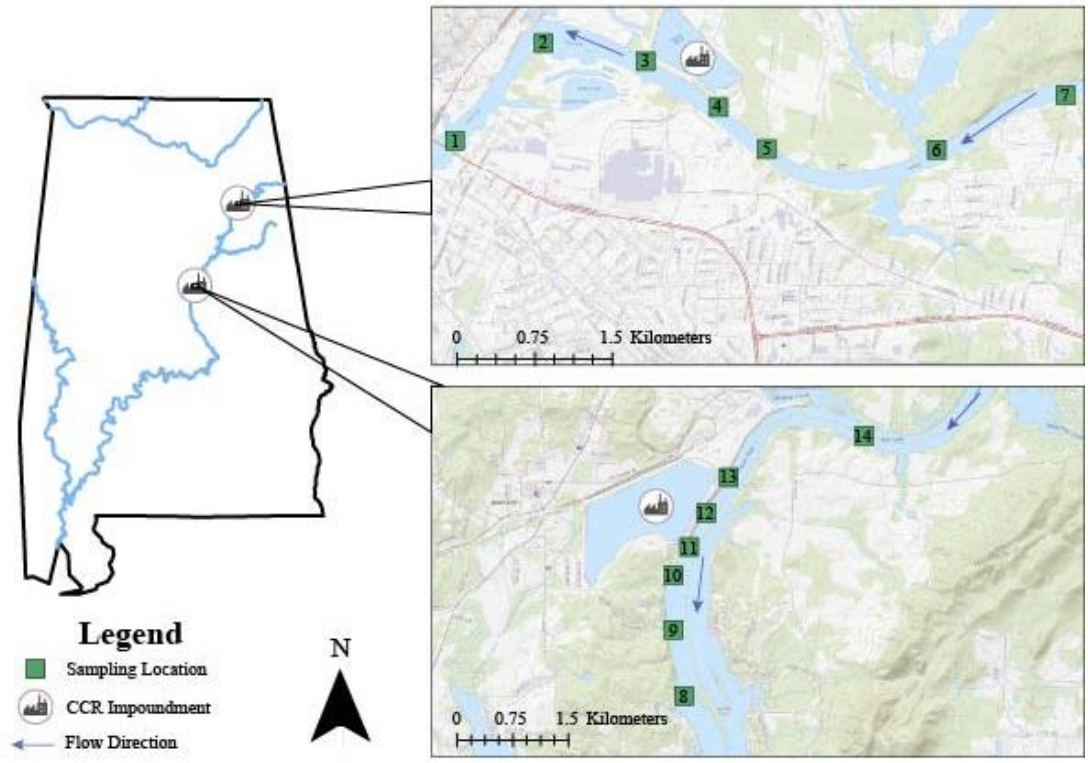

Figure 12: Spatial distribution of sample sites across the Coosa and the state of Alabama.

Sources: USGS The National Map: National Boundaries Dataset, National Elevation Dataset, Geographic Names Information System, National Hydrography Dataset, National Land Cover Database National Structures Dataset, and National Transportation Dataset; U.S. Census Bureau- Tiger/Line

2.2.2 Sample Collection

One field trip was conducted on December 14th, 2021; assistance with boat operation and sample collection was completed by Troy Clift and the Waters' Paleolimnology Lab at Auburn University. At each impoundment, water and sediment samples were collected upstream (n=2), adjacent to (n=3), and downstream (n=2) of each facility. Water samples were collected using a Van Dorn water sampler and stored in high-density polyethylene bottles. Sediment samples were collected using a Van Veen grab sampler. Water and sediment samples were stored on ice in a cooler during sampling (~0°C) and transportation back to Auburn University and stored for analysis at 4 °C.

2.2.3 Sample Preparation and Analysis

After transportation, water samples were filtered using a 0.45 µm cellulose filter and acidified dropwise to a pH of 2 using 3M nitric acid (Ward's Science, USA). Large organic debris was initially removed from all sediment samples. Sediment sample preparation was followed EPA Method 200.2. Roughly 20-100 grams of sediment were oven dried at 60 °C for 3-5 days. Weights were recorded each day. Dried sediments were sieved using a size 6 sieve then transferred to a mortar, sediments were manually ground with a pestle to achieve homogeneity. The mortar was cleaned with acetone and ultrapure water (18.2 Ω; Micropore System Thermo Scientific, USA) between each sample to limit cross contamination.

2.2.4 Sediment Digestion and Analysis

Sediment acid digestion and metal analysis was performed by University of Georgia Laboratory of Environmental Analysis. The microwave assisted nitric digestion followed EPA Method 3052 for sediment digestion. Trace metals V, Cr, Fe, Mg, Ca, Ni, As, Cu, Se, Sr, Mo, Sb,

Pb, Tl were quantified in the sediment using ICP-MS and reported in ppb and ppm for surface water and sediment samples respectively. A NIST standard, NIST 1633c: Trace Elements in CCR was prepared in the same manner described above and analyzed in triplicate with sediment samples.

Enrichment factors, shown in EQ 1, were calculated for each element of interest in both the water and sediment samples. Sample site 7, the most upstream site, was used as the pristine site for this study.

$$Enrichment\ Factor = \frac{Concentration\ of\ Element_{sample\ site}}{Concentration\ of\ Element_{pristine\ site}} \quad \text{(EQ 1)}$$

2.3 Results

2.3.1 Enrichment Factors

Mixing of CCR with sediments and surface water results in enrichment of major ions and heavy metals (Harkness et al., 2016; Ruhl et al., 2012; Vengosh et al., 2019). Enrichment by two to three levels of magnitude of trace elements, specifically Cu, As, Se, Mo, Sr, Sb, and Tl, have been utilized as CCR contamination signature. In this study, the CCR standard (Figure 13, black dotted line) produced similar enrichment pattern, as the one produced in Vengosh et al., (2019), demonstrating that it is relatively unimpacted reference material. Enrichment factors of sediment and surface water samples from this study were calculated against the most upstream site, site 7, and are shown in Figures 13 and 14, respectively. Highest sediment enrichment factors were 16.24 (Mo) and 15.60 (Sr) at Gadsden Site 1 and Gaston Site 13, respectively. Sediment enrichment factors did not exhibit enrichment trends similar to that of the CCR standard.

In surface water samples, there was a high Mo enrichment of 39.89 upstream of the Gaston (Gaston 13); this enrichment decreased with distance downstream until reaching the enrichment factor of 4.36 at the most downstream site (Gaston 8). The highest surface water enrichment factors of the other trace elements include 2.56 (Ni) and 4.90 (Se) at Gadsden 3 and Gaston 13 respectively.

2.3.2 Linear Relationship between Antimony and Molybdenum

Significant linear relationships between trace elements of interest, e.g. Se, As, Sb, and Mo, have been used as another line of evidence of CCR contamination (Vengosh et al., 2019). In this study, linear relationships between Sb and Mo are shown in Figure 15 for sample sites downstream and adjacent to CCR impoundments. Strong correlations between Mo and Sb were observed in

both sediment (R^2=0.8758) and surface water samples (R^2=0.8215), suggesting CCR impacted water and sediment. In contrast, strong linear relationships were not observed between As and Se in sediment and surface water samples, Figure 19 in Appendix.

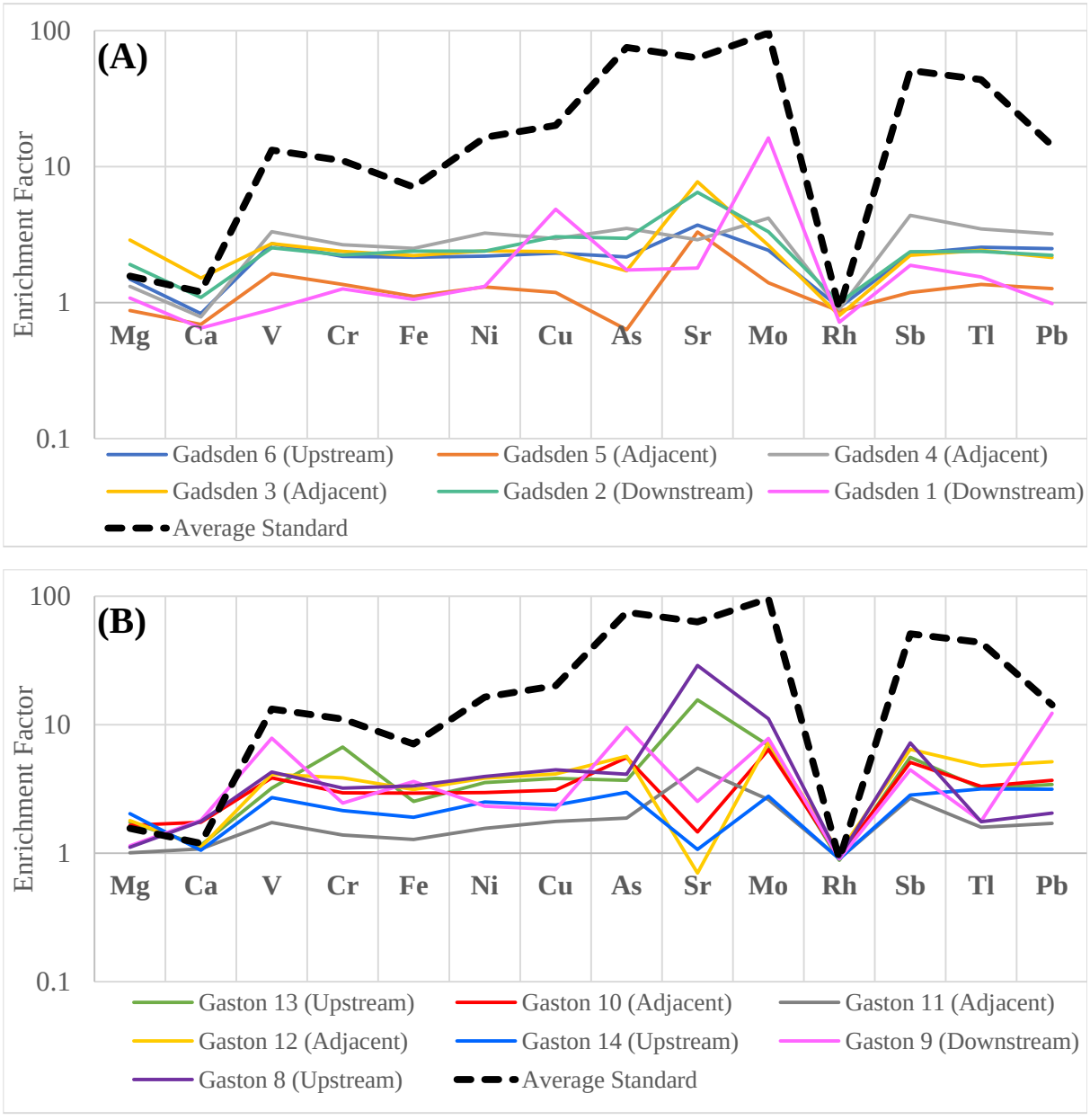

Figure 13: Distribution and enrichment of trace elements of sediment samples collected nearby the Gadsden (A) and Gaston (B) CCR impoundment. The most upstream site, Gadsden 7, was used as a reference for calculating enrichment values. Black dash line represents enrichment values of CCR standard (NIST 1633c)

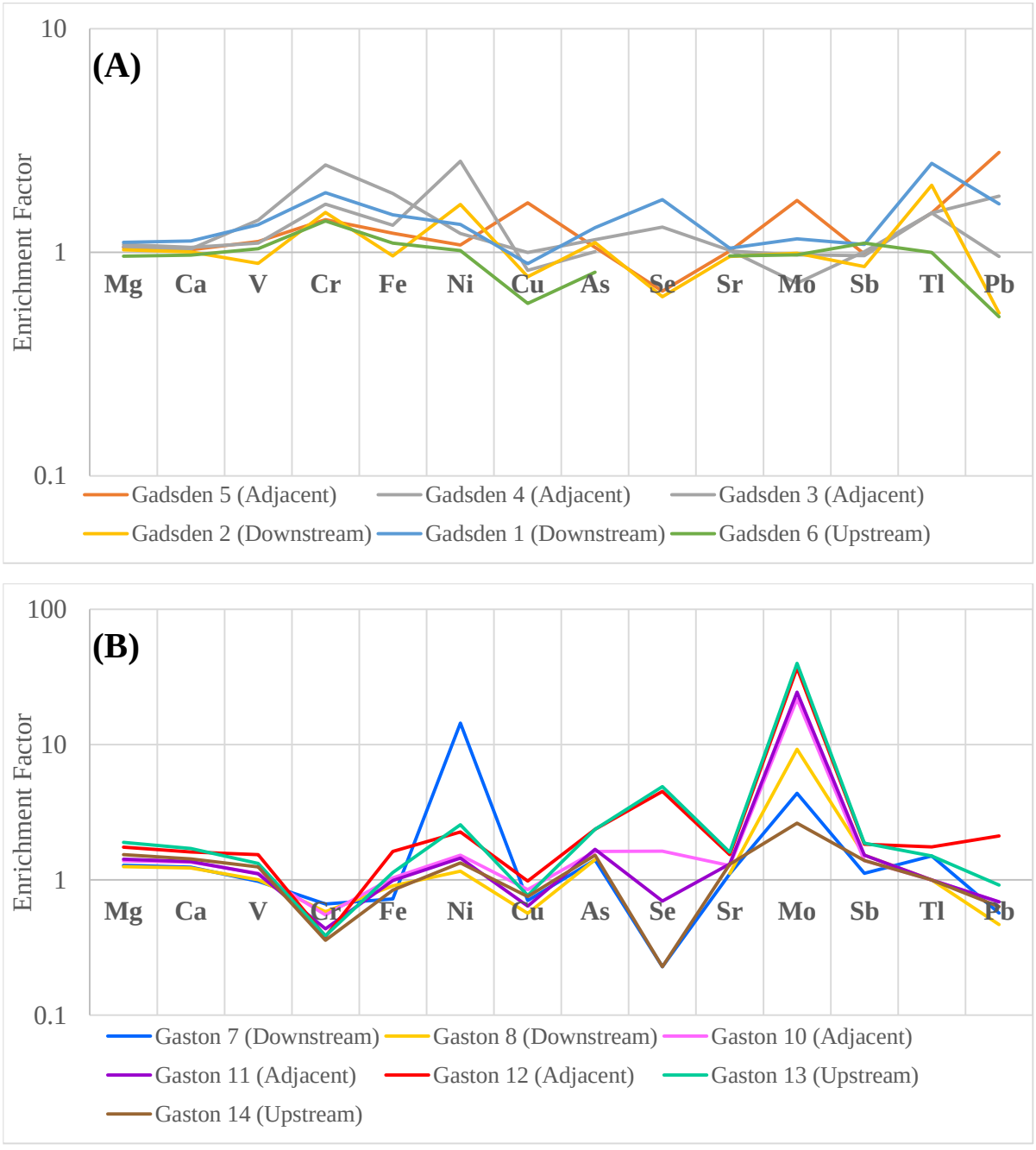

Figure 14: Distribution and enrichment of trace elements in surface water samples collected nearby the Gadsden (A) and Gaston (B) CCR impoundment. The most upstream site, Gadsden 7, was used as a reference for calculating enrichment values.

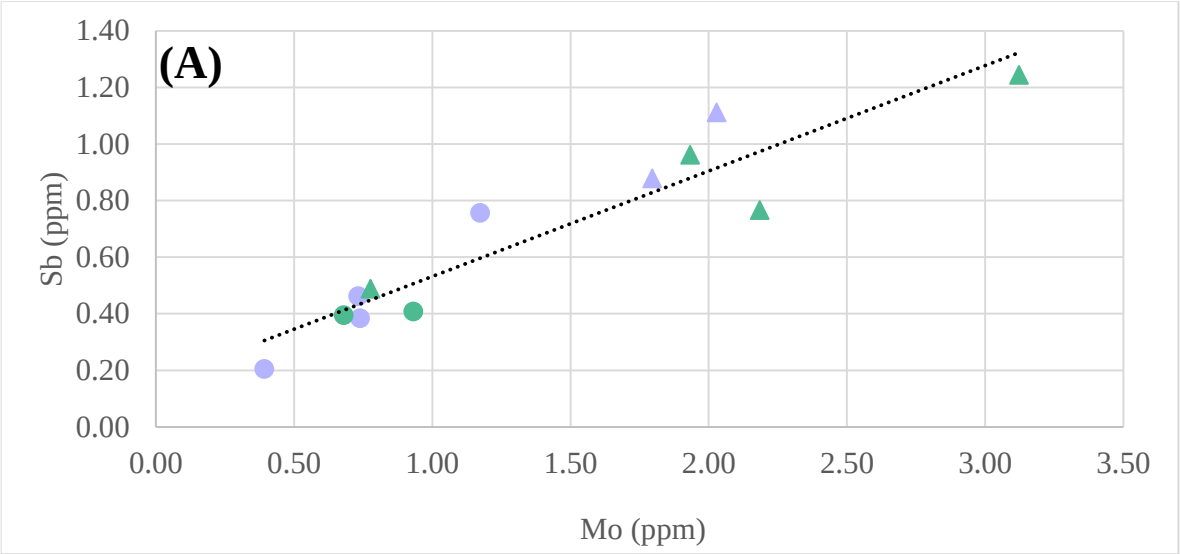

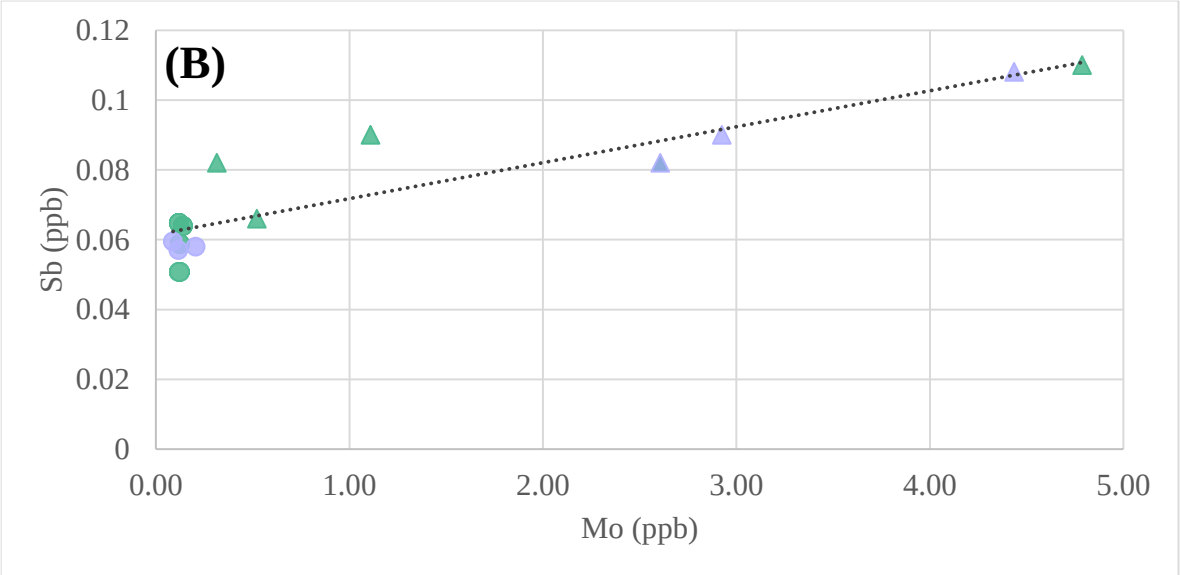

Figure 15: Linear relationship of antimony (Sb) and Molybdenum (Mo) in surface water samples. Gaston samples are represented by triangles; Gadsden samples are represented by circles. Samples adjacent to the impoundments are indicated in purple; all other samples are denoted in green.

2.4 Discussion

Enrichment factors for sediment did not match the behavior observed in the CCR standard. Additionally, enrichment factors were not as elevated as levels reported in previously publications on CCR contamination. For example, Vengosh et al., (2019) found enrichment factors up to 100 for Se, Mo and Sb, while in this study, the enrichment values were below 10 for most elements studied. Although the strong linear relationship between Mo and Sb was found in sediment and surface water samples, a linear relationship was not observed between As and Se. Together, the data present is not strong enough evidence to determine if CCR is leaching into surface water.

2.4.1 Molybdenum

Surface water samples in proximity to the Gaston CCR impoundment indicate elevated levels of Mo. Although the data collected is not enough to suggest the source is from CCR contamination, it presents the opportunity for additional research ventures. Mo concentrations have historically been elevated for the Gaston impoundment with Southern Company issuing a notice of groundwater protection standard exceedance for Mo in 2018 (Wallis, 2018). It must be mentioned that additional trace elements were included on the groundwater protection standard exceedances, including As, lithium (Li), and radium (Ra), but in this study, maximum As enrichment only reached values of 9.55 and 2.37 for sediment and surface water samples respectively. Considering geogenic Mo originates from molybdenite, granite, metagranite, and metasomatic rock, the surrounding geology.

Considering geogenic Mo originates from molybdenite, granite, metagranite, and metasomatic rock, the surrounding geology is unlikely responsible for the enrichment of Mo in proximity to the Gaston impoundment. The Gaston and Gadsden CCR impoundments are both located in the Coosa Valley district of the Valley and Ridge physiographic province (Southern

Company Services Earth Science and Environmental Engineering, 2022a, 2019). At the Gadsden impoundment site, the site geology includes Quaternary-age alluvial low and high terrace deposits and the Conasauga Formation, consisted of varying amounts of limestone, dolomite and shale (Southern Company Services Earth Science and Environmental Engineering, 2019). The subsurface bedrock geology of the Gaston impoundment consist mainly of dolomites from the Knox Group (Southern Company Services Earth Science and Environmental Engineering, 2022b).

Although CCR is the primary source of anthropogenic Mo, additional point sources to be considered include municipal sewage sludge, non-ferrous metal smelting, and mining operations (Barceloux, 1999; Chappaz et al., 2008). Additional research is required to understand if Mo is originating from the CCR impoundment and what geochemical processes allow Mo to leak through the constructed reactive barrier of the impoundment while other metals are retained.

2.4.2 Limitations

The sampling design of this experiment may have been of the largest limitations of this study. Only seven samples were able to be collected at each site with replicates of two upstream and downstream and replicates of three adjacent to the impoundment. Increasing the sample size and increase the spatial distribution of samples sites would have greatly benefited this study. The reference site of Vengosh et al., (2019) was reservoir that was not located within the same watershed as the sample sites. An impacted pristine site could cause the enrichment factors to be depressed.

2.4.3 Future Directions

Additional indicators of CCR contamination are planned to be investigated. One primary CCR signature analysis to be completed is detection of CCR particles in sediment samples. CCR

particles have such an unique morphology which has been used as a tool to determine CCR mixing with natural sediments (Brown et al., 2011; Vengosh et al., 2019; Wang et al., 2020). With Field Emission-Scanning Electron Microscopy, the percent of identified fly ash can be identified and counted as another line of evidence of CCR contamination in the area (Brown et al., 2011; Vengosh et al., 2019). Elevated levels of low field magnetic susceptibility, another diagnostic CCR indicator, could also be used to determine CCR exposure in sediment samples (Wang et al., 2020).

This study focused on two impoundment facilities; seven other facilities exist within the state of Alabama(Sackett, 2015). A more extensive study should be conducted to understand the potential CCR contamination throughout the entire state of Alabama.

2.5 Conclusion

Evidence collected in this study is not strong enough to support the hypothesis of CCR contributing to reduce water quality in the Coosa River. Additional diagnostic tracers should be investigated should completed to conclusive determine if there is CCR contamination within the Coosa River. We hope this is a preliminary study that stimulates a more extensive on CCR contamination within the state of Alabama.

3. Appendix

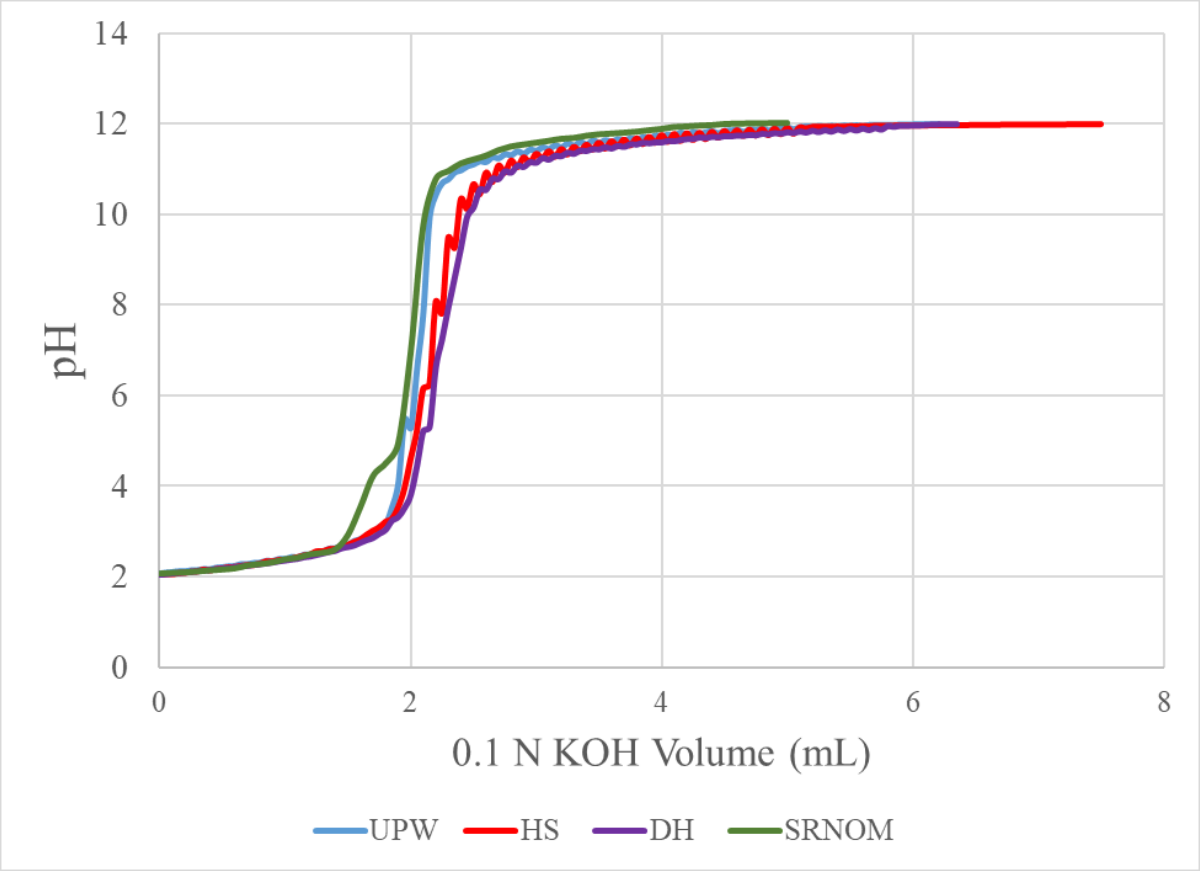

Figure 16: Titration curves of DOM standards, HS (red), DH (purple), and SRNOM (green) and UPW (blue)

Table 3: Functional group content of DOM standards

	DH	HS	SRNOM
Carboxyl Group Content (mmol/g)	0.15	0.125	0.15
Phenolic Group Content (mmol/g)	0.05	0.05	0.05

Table 4: Mass balance of equilibrium dialysis experiments

Theoretical As In				As Out/Measured					
DOM Type	Treatment (ppb)	As Added From Standard (µg)	Background As from DOM (µg)	Inside Tube (ppb)	Total As Inside (µg)	Outside tube (ppb)	Total As Outside (µg)	Complete Total of Measured As (µg)	Complete - Theoretical (%)
HS	500	16.00	0.01	2607.00	78.21	275.50	137.75	215.96	1248%
HS	100	3.10	0.02	148.90	4.62	58.19	29.10	33.71	981%
HS	50	1.70	0.02	38.62	1.31	36.00	18.00	19.31	1024%
HS	10	0.32	0.02	0.52	0.02	0.69	0.35	0.36	8%
HS	5	0.15	0.01	0.62	0.02	0.47	0.24	0.25	58%
HS	0	0.00	0.02	0.46	0.01	0.42	0.21	0.22	1354%
HS	500	15.00	0.02	41.62	0.62	28.50	14.25	14.87	-1%
HS	100	3.26	0.02	8.24	0.13	5.85	2.92	3.06	-7%
HS	50	1.50	0.01	2.98	0.05	1.93	0.96	1.01	-33%
HS	10	0.30	0.01	1.96	0.06	0.48	0.24	0.30	-5%
HS	5	0.13	0.01	0.70	0.02	0.28	0.14	0.16	8%
HS	0	0.00	0.17	0.188	0.07	BDL*	0.005	0.07	-59%
SRNOM	0	0	0.02	BDL*	0.00037	BDL*	0.005	0.01	-71%
SRNOM	0	0	0.00465	0.23	0.00828	0.28	0.14	0.15	3089%
SRNOM	5	0.2	0.00	1.0	0.0	0.2	0.116	0.15	-19%
SRNOM	5	0.2	0.01	0.9	0.0	0.4	0.215	0.25	26%
SRNOM	10	0.3	0.00	0.5	0.0	0.6	0.289	0.31	-6%
SRNOM	10	0.4	0.00	4.0	0.1	0.5	0.225	0.4	0%
SRNOM	50	1.8	0.00	33.7	1.2	29.9	14.97	16.15	819%
SRNOM	50	1.9	0.00	55.6	2.1	30.2	15.08	17.14	824%
SRNOM	100	3.0	0.00	6.3	0.2	5.6	2.82	3.009	0%
SRNOM	100	3.7	0.00	113.4	4.2	61.3	30.63	34.823	840%
SRNOM	500	15.0	0.00	32.2	1.0	24.3	12.125	13.09	-13%
SRNOM	500	19.5	0.01	481.2	18.8	341.1	170.55	189.32	871%
SRNOM	100	3.2	0.01	70.25	3.0	67.4	33.695	36.69	1045%
SRNOM	50	1.7	0.00	42.87	1.0	36.9	18.44	19.44	1017%
SRNOM	0	0	0.01	0.41	BDL*	0.4	0.19	0.21	3895%
DH	500	4.94	0.01	1.15	0.02	12.81	6.41	6.42	30%
DH	100	1.00	0.01	3.63	0.06	2.93	1.47	1.52	51%
DH	50	0.50	0.01	2.79	0.04	1.40	0.70	0.74	46%
DH	10	0.30	0.02	0.68	0.02	0.31	0.15	0.17	-45%
DH	5	0.17	0.02	0.32	BDL*	0.03	BDL*	0.02	-87%
DH	0	0.00	0.02	0.064	0.00	0.044	0.02	0.02	24%
Blank	500	14.00	0.00	269.6	7.55	263.2	131.60	139.15	894%
Blank	100	3.30	0.00	70.45	2.32	69.62	34.81	37.13	1027%

*BDL acronym denotes As concentrations below the detection limit

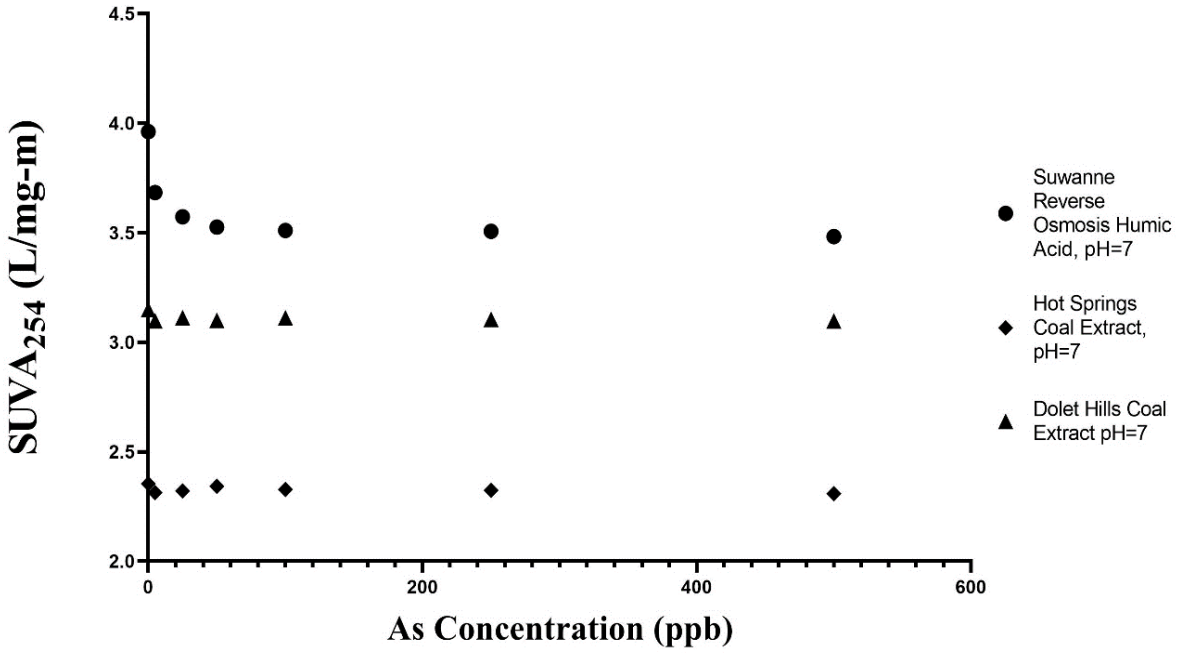

Figure 17: Measurements of SUVA 254 with As addition (0-500 ppb) at a pH of 7 with three different types of DOM: Suwanne Reverse Osmosis (circle), HS (diamond), and DH (triangle).

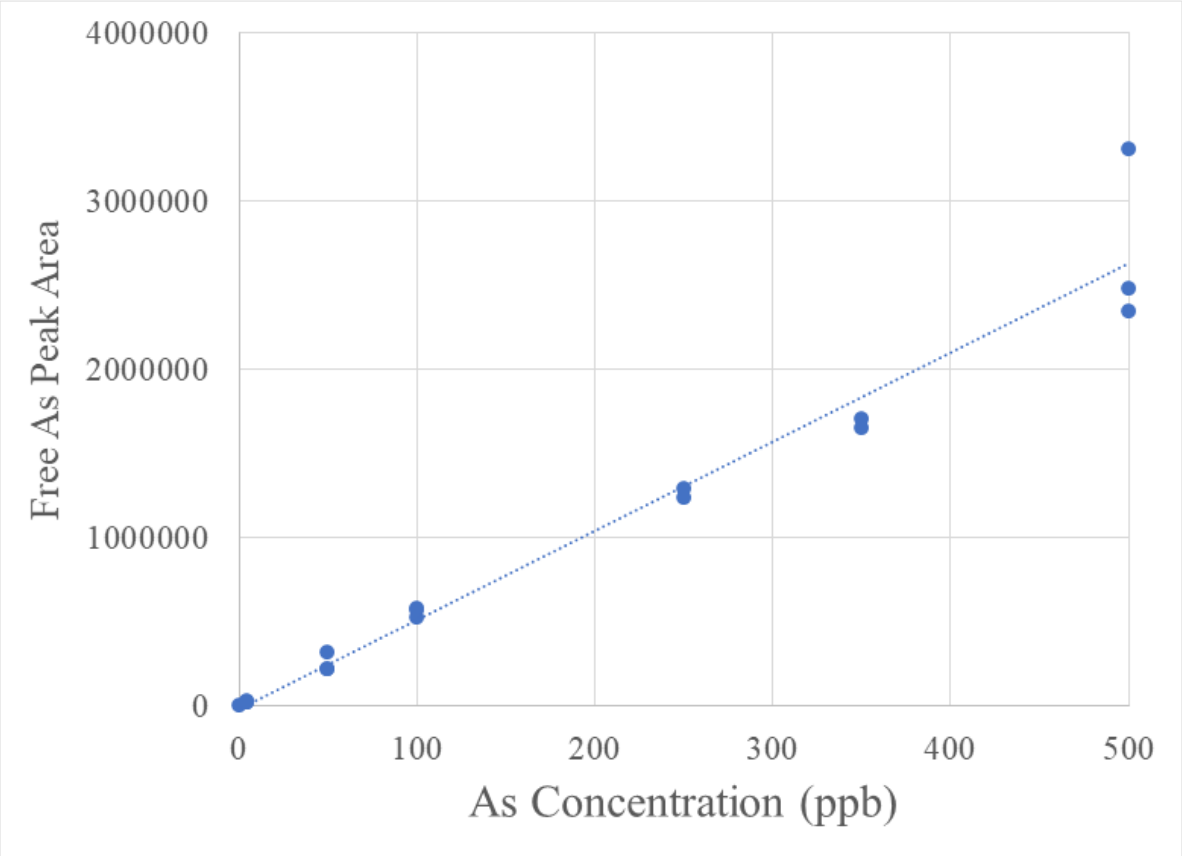

Figure 18: Calibration curve of HPLC-SEC-ICP-MS analysis using sodium arsenite standards in UPW (R^2=0.9612)

Table 5:Statistical analysis of the calibration curve for HPLC-SEC-ICPMS analysis of sodium arsenite standards in UPW

As Concentration (ppb)	Free As Peak Area	Standard Deviation	Relative Standard Deviation
0	0	0	0
5	24890	5461.0	0.219403848
50	258324	58638.9	0.226997567
100	558974	27964.7	0.050028599
250	1142907.067	207896.2	0.181901216
350	1635583.333	76234.5	0.046609981
500	2709104	522998.7	0.193052307

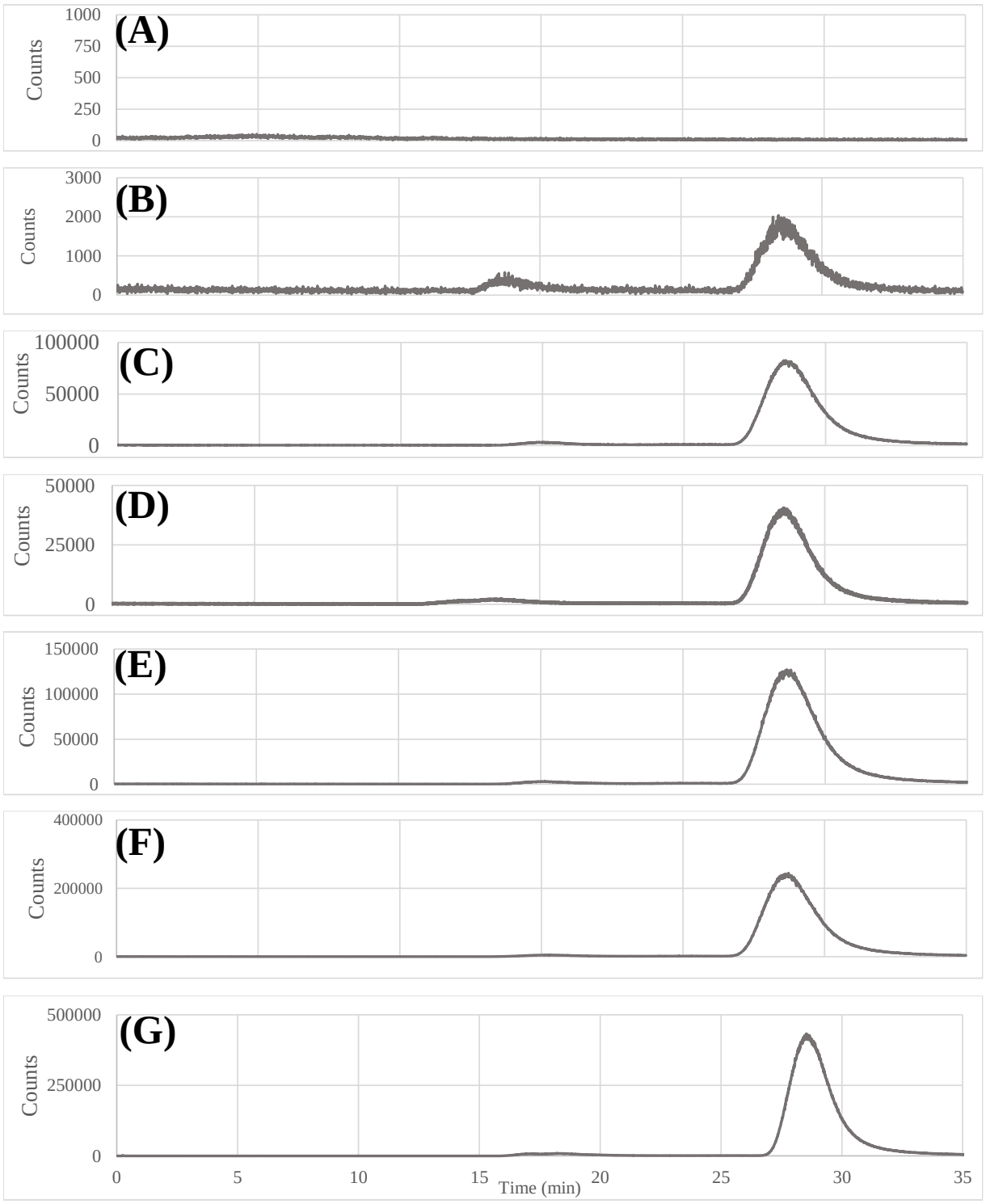

Figure 1919: HPLC-SEC-ICP-MS (gray line) chromatographs of As complexation with 18.2 Ω ultrapure water. The As treatments ranged from 0-500 ppb As: 0 (A), 5 (B), 50 (C), 100, (D), 250 (E), 350 (F), and 500 ppb (G).

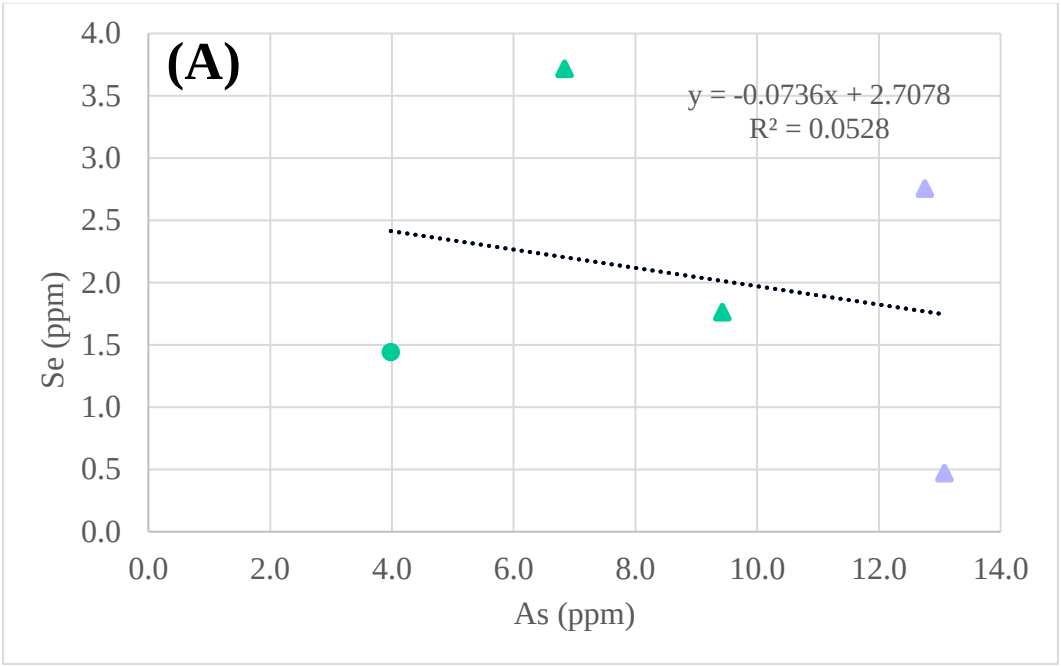

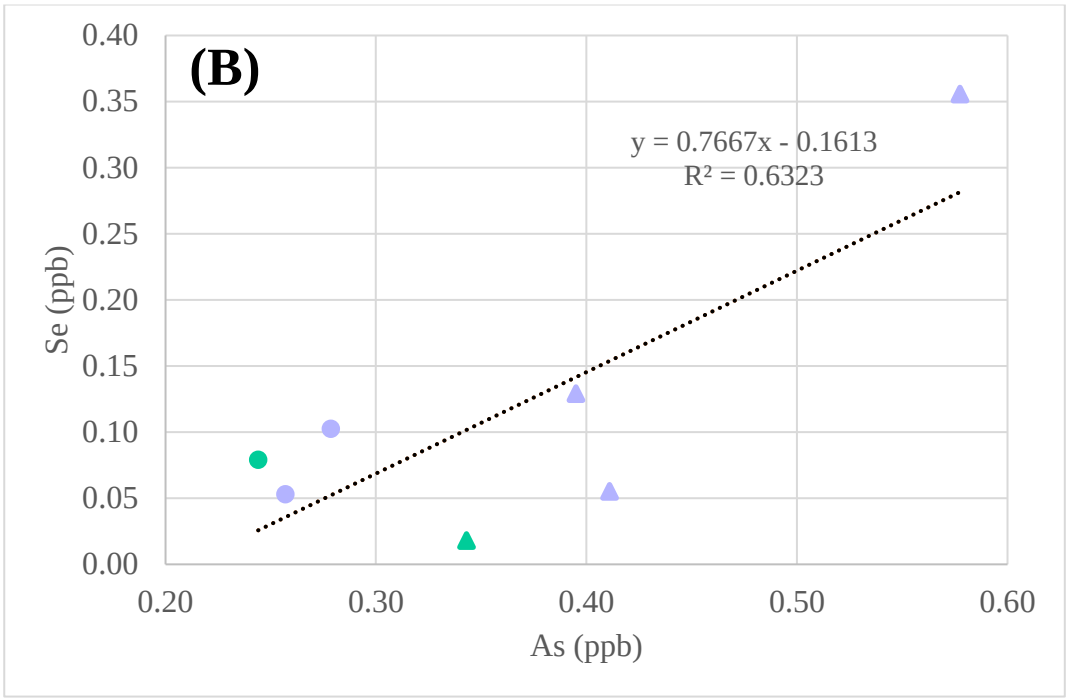

Figure 2020: Linear relationship of arsenic (As) and selenium (Se) in surface water samples. Gaston samples are represented by triangles; Gadsden samples are represented by circles. Samples adjacent to the impoundments are indicated in purple; all other samples are denoted in green

4. References

Aguirre, A., 2019. Applying Ge/Si Ratios to Trace Weathering Reactions, Hydrologic Pathways and Coal Fly Ash Contamination in Watershed Across the United States. Cornell University. Cornell.

Al-Reasi, H.A., Wood, C.M., Smith, D.S., 2013. Characterization of freshwater natural dissolved organic matter (DOM): Mechanistic explanations for protective effects against metal toxicity and direct effects on organisms. Environment International. 59, 201–207. https://doi.org/10.1016/j.envint.2013.06.005

American Coal Ash Association, 2018. ACAA 2018 CCP Survey Results. Farminton Hills, MI.

American Road & Transportation Builders Association, 2015. Production and Use of Coal Combustion Products in the U.S. - Market Forecast Through 2033, American Coal Ash Association.

Ayotte, J.D., Medalie, L., Qi, S.L., Backer, L.C., Nolan, B.T., 2017. Estimating the High-Arsenic Domestic-Well Population in the Conterminous United States. Environmental Science and Technology. 51, 12443–12454. https://doi.org/10.1021/acs.est.7b02881

Barceloux, D.G., 1999. Molybdenum. Journal of Toxicol. - Clinical Toxicol. 37, 231–237. https://doi.org/10.1081/CLT-100102422

Bauer, M., Blodau, C., 2009. Arsenic distribution in the dissolved, colloidal and particulate size fraction of experimental solutions rich in dissolved organic matter and ferric iron. Geochimica et Cosmochimic Acta. 73, 529–542. https://doi.org/10.1016/j.gca.2008.10.030

Brown, P., Jones, T., BeruBe, K., 2011. The interal microstructure and fibrous mineralogy of fly ash from coal-burning power stations. Environmental Pollution. 159, 3324–3333.

Buschmann, J., Kappeler, A., Lindauer, U., Kistler, D., Berg, M., Sigg, L., 2006. Arsenite and

Arsenate Binding to Dissolved Humic Acids : Influence of pH , Type of Humic Acid , and Aluminum. Environmental Science and Technology. 40, 6015–6020.

CCR Rule Compliance Data and Information, 2022. Alabama Power Company. https://www.epa.gov/coalash/effort-assess-coal-combustion-residuals-ccr-disposal-units#assessments

Chappaz, A., Gobeil, C., Tessier, A., 2008. Geochemical and anthropogenic enrichments of Mo in sediments from perennially oxic and seasonally anoxic lakes in Eastern Canada. Geochimica et Cosmochimica Acta. 72, 170–184. https://doi.org/10.1016/j.gca.2007.10.014

Coal Ash Issues in Alabama, 2014. South. Alliance Clean Energy.

Desoye, G., 1988. Error analysis in equilibrium dialysis : evaluation of adsorption phenomena. Journal of Biochemical and Biophysical Methods 17, 3–16.

Dowling, C.B., Poreda, R.J., Basu, A.R., Peters, S.L., 2002. Geochemical Study of Arsenic Release Mechanisms in the Bengal Basin Groundwater Geochemical study of arsenic release mechanisms in the Bengal Basin groundwater. Water Resources Research. 38 (0), 1-20https://doi.org/10.1029/2001WR000968

Effort to Assess Coal Combustion Residuals (CCR) Disposal Units, 2022. . United States Environmental Protection Agency.

Focazio, M., Welch, A., Watkins, S., Helsel, D., Horn, M., 2000. A Retrospective Analysis on the Occurence of Arsenic in Ground-Water Resources of the United States and Limitations in Drinking-Water-Supply Characterization, U.S.G.S. Water-Resources Investigations Report 99-4279.

Gao, Y., Yan, M., Korshin, G. V, 2015. Effects of Ionic Strength on the Chromophores of Dissolved Organic Matter. Environmental Science and Technology. 49, 5905–5912.

https://doi.org/10.1021/acs.est.5b00601

Harkness, J.S., Sulkin, B., Vengosh, A., 2016. Evidence for Coal Ash Ponds Leaking in the Southeastern United States. Environmental Science and Technology. 50, 6583–6592. https://doi.org/10.1021/acs.est.6b01727

International Humic Substances Society. Elemental Compositions and Stable Isotopic Ratios of IHSS Samples]. 2022. URL https://humic-substances.org/elemental-compositions-and-stable-isotopic-ratios-of-ihss-samples/ (accessed 5.8.22).

Lemly, A.D., Skorupa, J.P., 2013. Wildlife and the coal waste policy debate: Proposed rules for coal waste disposal ignore lessons from 45 years of wildlife poisoning. Environmental Science and Technology. 47, 11367–11368. https://doi.org/10.1021/es403359z

Li, P., Hur, J., 2017. Utilization of UV-Vis spectroscopy and related data analyses for dissolved organic matter (DOM) studies: A review. Crit. Rev. Environmental Science and Technology. 47, 131–154. https://doi.org/10.1080/10643389.2017.1309186

Li, X., Guo, H., Zheng, H., Xiu, W., He, W., Ding, Q., 2019. Roles of different molecular weights of dissolved organic matter in arsenic enrichment: Evidences from ultrafiltrations and EEM-PARAFAC. Applied Geochemistry 104, 124–134.

Lin, H.T., Wang, M.C., Li, G.C., 2004. Complexation of arsenate with humic substance in water extract of compost. Chemosphere 56, 1105–1112. https://doi.org/10.1016/j.chemosphere.2004.05.018

Liu, G., Cai, 2014. Studying Arsenite-Humic Acid Complexation Using Size Exclusion Chromatography-Inductively Coupled Plasma Mass Spectrometry. Journal of Hazardous Materials. 262, 1223–1229. https://doi.org/10.1016/j.jhazmat.2012.05.043.Studying

Liu, G., Cai, Y., 2010. Complexation of Arsenite with Dissolved Organic Matter: Conditional

Distribution Coefficients and Apparent Stability Constants. Chemosphere 81, 890–896. https://doi.org/10.1016/j.chemosphere.2010.08.002.Complexation

Liu, G., Fernandez, A., Cai, Y., 2011. Complexation of Arsenite with Humic Acid in the Presence of Ferric Iron. Environmental Science and Technology. 45, 3210–3216. https://doi.org/10.1021/es102931p

Malcolm, R.L., MacCarthy, P., 1986. Limitations in the Use of Commercial Humic Acids in Water and Soil Research. Environmental Science and Technology. 20, 904–911. https://doi.org/10.1021/es00151a009

Malina, N., Olshansky, Y., Ojeda, A.S., 2022. Role of dissolved organic matter molecular weight in iron (III) complexation in water. (*in preparation*)

McDonough, L.K., Andersen, M.S., Behnke, M.I., Rutlidge, H., Oudone, P., Meredith, K., Carroll, D.M.O., Santos, I.R., Marjo, C.E., Spencer, R.G.M., Mckenna, A.M., Baker, A., 2022. A new conceptual framework for the transformation of groundwater dissolved organic matter. Nature Communications. 1–11. https://doi.org/10.1038/s41467-022-29711-9

Miller, M.P., Simone, B., Hageman, C., Rahman, M.M., Mcknight, D.M., 2010. Dissolved Organic Matter Sources and Consequences for Iron and Arsenic Mobilization in Bangladesh Aquifers. Environmental Science and Technology. 44, 123–128.

Ojeda, A.S., Ford, S.D., Gallucci, R.M., Ihnat, M.A., Philp, R.P., 2019. Geochemical characterization and renal cell toxicity of water-soluble extracts from U . S . Gulf Coast lignite. Environmental Geochemistry and Health 41, 1037–1053. https://doi.org/10.1007/s10653-018-0196-7

Progotir Pothey, 2015. Bangladesh: Multiple Indicator Cluster Survey 2012–2013: Final Report, Bangladesh Bureau of Statistics (BBS) and United Nations Children's Fund (UNICEF).

Dhaka, Bangladesh.

Redman, A.D., Macalady, D.L., Ahmann, D., 2002. Natural Organic Matter Affects Arsenic Speciation and Sorption onto Hematite. Environmental Science and Technology l. 36, 2889–2896.

Ren, J., Fan, W., Wang, X., Ma, Q., Li, X., Xu, Z., Wei, C., 2017. Influences of size-fractionated humic acids on arsenite and arsenate complexation and toxicity to Daphnia magna. Water Research. 108, 68–77. https://doi.org/10.1016/j.watres.2016.10.052

Ritter, K., Aiken, G.R., Ranville, J.F., Bauer, M., Macalady, D.L., 2006. Evidence for the Aquatic Binding of Arsenate by Natural Organic Matter - Suspended Fe (III). Environmental Science and Technology. 40, 5380–5387. https://doi.org/10.1021/es0519334

Ruhl, L., Vengosh, A., Dwyer, G.S., Hsu-kim, H., Schwartz, G., Romanski, A., Smith, S.D., 2012. The Impact of Coal Combustion Residue Effluent on Water Resources: A North Carolina Example. Environmental Science and Technology. 46, 12226–12233. https://doi.org/10.1021/es303263x

Sackett, J., 2015. Alabama Drinking Water Supplies Downstream from Coal Ash Impoundments. South. Environ. Law Cent. http://www.southeastcoalash.org/wp-content/uploads/2015/03/Drinking_Water_Supplies_and_CoalAsh_AL_Map_2015_0304.pdf (accessed 8.7.22).

Selinus, O. (Ed.), 2013. Essentials of Medical Geology, 1st ed. Springer Dordrecht. https://doi.org/https://doi.org/10.1007/978-94-007-4375-5

Sharma, V.K., Sohn, M., 2009. Aquatic arsenic: Toxicity, speciation, transformations, and remediation. Environmental International. 35, 743–759. https://doi.org/10.1016/j.envint.2009.01.005

Smedley, P.., Kinniburgh, D.G., 2002. A review of the source, behaviour and distribution of arsenic in natural waters RN - Appl. Geochem., vol. 17, pp. 517-568. Applied Geochemistry 17, 517–568.

Southern Company Services Earth Science and Environmental Engineering, 2022. 2021 ANNUAL GROUNDWATER MONITORING AND CORRECTIVE ACTION REPORT ALABAMA POWER COMPANY.

Southern Company Services Earth Science and Environmental Engineering, 2019. 2018 Annual & 2019 First Semi-annual Groundwater Monitoring and Corrective Action Report. Alabama Power Co. 1–1900.

Stevenson, F.J., 1994. Humus Chemistry: Genesis, Composition, Reactions, Second Edi. ed. John Wiley & Sons, New York, NY.

Tadini, A.M., Moreira, A.B., 2014. Fractionation of Aquatic Humic Substances and Dynamic of Chromium Species in an Aquatic Body Influenced by Sugarcane Cultivation. Journal of Brazalian Chemical Society. 25, 119–125. https://doi.org/10.5935/0103-5053.20130277

Tipping, E., 2002. Cation Binding by Humic Substances. Cambridge University Press. https://doi.org/10.1017/CBO9780511535598

Vengosh, A., Cowan, E.A., Coyte, R.M., Kondash, A.J., Wang, Z., Brandt, J.E., Dwyer, G.S., 2019. Evidence for unmonitored coal ash spills in Sutton Lake, North Carolina : Implications for contamination of lake ecosystems. Science of the Total Environment. 686, 1090–1103. https://doi.org/10.1016/j.scitotenv.2019.05.188

Wallis, E., 2018. Notice of Groundwater Protection Standard Exceedance - Gaston Gypsum Pond.pdf.

Wang, N., Sun, X., Zhao, Q., Yang, Y., Wang, P., 2020. Leachability and adverse effects of coal

fly ash: A review. Journal of Hazardous Materials. 396, 1–26. https://doi.org/10.1016/j.jhazmat.2020.122725

Wang, Z., Dwyer, G.S., Coleman, D.S., Vengosh, A., 2019. Lead Isotopes as a New Tracer for Detecting Coal Fly Ash in the Environment. Environmental Science and Technology Letters. 6, 714–719. https://doi.org/10.1021/acs.estlett.9b00512

Weishaar, J.L., Fram, M.S., Fujii, R., Mopper, K., 2003. Evaluation of Specific Ultraviolet Absorbance as an Indicator of the Chemical Composition and Reactivity of Dissolved Organic Carbon. Environmental Science. 37, 4702–4708.

Zhang, F., Li, X., Duan, L., Zhang, H., Gu, W., Yang, X., Li, J., He, S., Yu, J., Ren, M., 2021. Effect of different DOM components on arsenate complexation in natural water. Environmental Pollution. 270, 116221. https://doi.org/10.1016/j.envpol.2020.116221

Zhang, S., Dai, S., Finkelman, R.B., Graham, I.T., French, D., Hower, J.C., Li, X., 2019. Leaching characteristics of alkaline coal combustion by-products: A case study from a coal-fired power plant, Hebei Province, China. Fuel 255, 115710. https://doi.org/10.1016/j.fuel.2019.115710